

Cite this: *Nanoscale*, 2024, **16**, 1471

# Organic iontronic memristors for artificial synapses and bionic neuromorphic computing

 Yang Xia,<sup>†a,b</sup> Cheng Zhang,<sup>†a</sup> Zheng Xu,<sup>a</sup> Shuanglong Lu,<sup>c</sup> Xinli Cheng,<sup>\*a</sup> Shice Wei,<sup>d</sup> Junwei Yuan,<sup>b</sup> Yanqiu Sun<sup>\*b</sup> and Yang Li<sup>†a,c</sup>

To tackle the current crisis of Moore's law, a sophisticated strategy entails the development of multistable memristors, bionic artificial synapses, logic circuits and brain-inspired neuromorphic computing. In comparison with conventional electronic systems, iontronic memristors offer greater potential for the manifestation of artificial intelligence and brain-machine interaction. Organic iontronic memristive materials (OIMs), which possess an organic backbone and exhibit stoichiometric ionic states, have emerged as pivotal contenders for the realization of high-performance bionic iontronic memristors. In this review, a comprehensive analysis of the progress and prospects of OIMs is presented, encompassing their inherent advantages, diverse types, synthesis methodologies, and wide-ranging applications in memristive devices. Predictably, the field of OIMs, as a rapidly developing research subject, presents an exciting opportunity for the development of highly efficient neuro-iontronic systems in areas such as in-sensor computing devices, artificial synapses, and human perception.

Received 28th November 2023,

Accepted 14th December 2023

DOI: 10.1039/d3nr06057h

rsc.li/nanoscale

<sup>a</sup>Jiangsu Key Laboratory of Micro and Nano Heat Fluid Flow Technology and Energy Application, School of Physical Science and Technology, Suzhou University of Science and Technology, Suzhou, Jiangsu 215009, China. E-mail: liyang@usts.edu.cn

<sup>b</sup>School of Chemistry and Life Sciences, Suzhou University of Science and Technology, Suzhou, Jiangsu 215009, China

<sup>c</sup>The Key Laboratory of Synthetic and Biological Colloids, Ministry of Education, Jiangnan University, Wuxi, Jiangsu 214122, China

<sup>d</sup>School of Microelectronics, Fudan University, Shanghai, 200433, China

†These authors contributed equally to this work.



Yang Li

Yang Li is an associate professor at the School of Physical Science and Technology, Suzhou University of Science and Technology. He received his BS and PhD degrees from Soochow University, under the supervision of Prof. Jianmei Lu. From 2016 to 2017, he got financial support from the Chinese government to complete his joint PhD research at Nanyang Technological University, in Prof. Qichun Zhang's group. He is currently a

Vebleo Fellow. His research interests focus on the preparation of novel organic/inorganic memristive materials and devices, and their applications for data storage and neuromorphic computing.

## 1. Introduction

The conventional von Neumann architecture, which has been the foundation for computing since its inception, segregates processing and memory units and thus results in a well-known bottleneck commonly referred to as the “von Neumann bottleneck”.<sup>1–3</sup> The bottleneck arising from the constant shuttle of data between the processing and memory units not only produces significant energy consumption but also imposes limitations on the computing speed.<sup>4,5</sup> The academia and industry are actively seeking alternative computing architectures to sustain the advancement of computational power, given the termination of Moore's law and the limitations in further transistor miniaturization.<sup>6–8</sup> The most promising alternative is neuromorphic computing, which draws inspiration from the human brain and integrates processing and memory into a unified entity.<sup>9,10</sup> The brain serves as the central processing unit, and it is known that information transmission only consumes about 10–20 W.<sup>11</sup> Therefore, scientists have replicated brain-inspired computing by developing new principle paradigms known as neuromorphic computing, which aim to emulate the cognitive functions observed in the human brain.

To the best of our knowledge, the human nervous system is comprised of over 86 billion neurons. As depicted in Fig. 1a, these neurons form an intricate network interconnected through synapses, facilitating the transmission of chemical mediators (e.g., Ca<sup>+</sup>, Na<sup>+</sup>, and K<sup>+</sup>) from presynaptic to postsynaptic terminals. Inspired by this, iontronics have emerged as

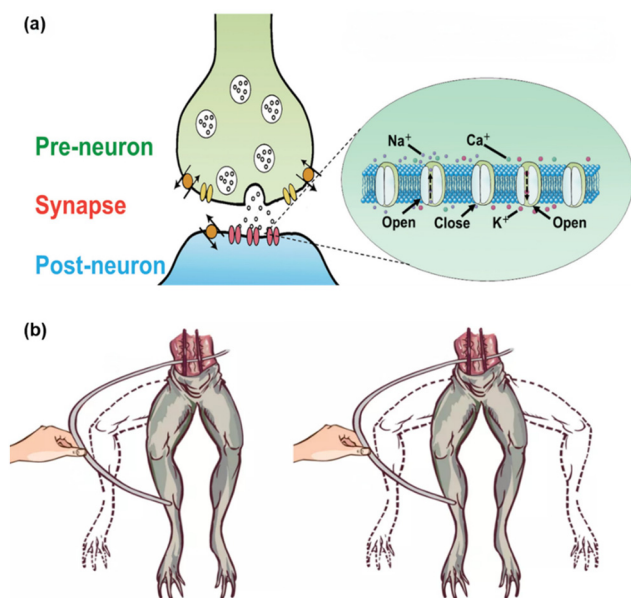


**Fig. 1** (a) Schematic image of an artificial synapse. (b) Stimulation of frog's leg muscles under electrical stimulation.<sup>47</sup> Reprinted with permission from ref. 47, © 2019 American Chemical Society.

an integral component in the field of electronics, affording the intricate interplay between ion regulation, coupled ion/electron charge transfer and signal exchange,<sup>12–14</sup> and exerting a significant influence in areas such as data storage and bionics.<sup>15,16</sup> As shown in Fig. 1b, the earliest studies of ion/electron coupling can be traced back to the galvanic frog muscle electrophysiological experiments in the 18th century, covering interdisciplinary subjects such as energy, sensing, and information transmission.<sup>17</sup> Afterward, investigation into these fundamental scientific issues, such as iontronic materials, ion/electron coupling interfaces, iontronic devices and so on, has established a solid groundwork for future ion/electron logic circuits and neuromorphic computing.<sup>18,19</sup>

The ionic-type organic semiconductor materials, which typically consist of electrovalent bonds and charged groups, possess distinct advantages and attract greater attention compared to conventional neutral organic functional materials.<sup>20,21</sup> These materials exhibit electron and ion conduction, providing enhanced functionalities like ion diffusion and adsorption, electrochemical activity, and tunable conductivity.<sup>22,23</sup> Besides, their high ion mobility, selectivity, and reversible redox make them ideal for multifunctional devices performing both electronic and ionic functions.<sup>24,25</sup> Therefore, ion-doped organic materials and their iontronic devices have been further applied to various areas, such as light-emitting devices (LEDs), field-effect transistors (FETs), sensors, and especially memristors and neuromorphic computing.<sup>26–32</sup> Accordingly, organic ionic memristive materials (OIMs) and memristive devices have emerged as new electronics relying on ion migration and electron permeation in the solid ion transport layer.<sup>33–36</sup> OIMs hold great promise in artificial intelligence (AI), neuromorphic computing, brain-

computer interfaces, *etc.* to enable information processing, recognition, memorizing and forgetting, learning, and decision-making.<sup>37–45</sup>

This review aims to summarize the development and status of various OIMs in the field of memristor and neuromorphic computing, which possess an organic backbone and exhibit stoichiometric ionic states. As a class of emerging memristive materials,<sup>46</sup> OIMs have garnered great attention due to their low cost, easy synthesis, high stability and ion/electron coupling properties. Here, we discuss in depth the progress and prospects of OIMs, including their inherent advantages, diverse types, synthesis methodologies, and wide-ranging applications in memristive devices, and propose their applications in highly efficient neuro-iontronic systems, such as in-sensor computing devices, artificial synapses, and human perception. However, the future challenges of OIMs in stability and reproducibility still need to be addressed, which are also summarized and discussed.

## 2. Organic iontronic memristive materials (OIMs)

### 2.1. Brief concept and advantages of OIMs

A plethora of inorganic memristive materials have been utilized to construct memristor devices, and continued to dominate the field of memristor preparation, due to their exceptional processing efficiency and immense storage capacity.<sup>47–51</sup> Nevertheless, they often lack sufficient functional groups to be modified for diverse functionalities. By contrast, OIMs exhibit simultaneous electronic and ionic conductivity, and have attracted considerable attention in recent years due to their simple tuning ability and potential for a wide range of electronic applications, particularly in the field of organic iontronic memristors.<sup>52,53</sup> Generally, these OIMs consist of skeletons embedded with charged ions, which confers additional advantages compared to traditional memristive materials.<sup>54</sup> As summarized in Fig. 2, the primary advantage of OIMs lies in their capability to address intricate issues and specific needs through appropriate structural and functional design, thereby solving challenges pertaining to energy conversion, sensing, memory, and logic applications.<sup>55</sup> Secondly, OIM-based memristors may exhibit enhanced energy efficiency in both operation and control.<sup>56</sup> Furthermore, due to their insensitivity to magnetic fields, OIMs enable effective mitigation of electromagnetic interference in high-frequency and high-density environments, distinguishing them from electronic devices.<sup>57</sup> Finally, the deformable and flexible properties of OIMs facilitate more natural and comfortable contact with the human body, inducing the prospects for intelligent applications, such as wearable devices, implantable devices, and smart surfaces. To sum up, OIMs possess the advantages of addressing complex problems, exhibiting low energy consumption, resisting interference, and facilitating seamless human–computer interaction,<sup>53,54,56</sup> and can serve as robust contenders for the development of innovative electronic devices and systems.<sup>58–60</sup>

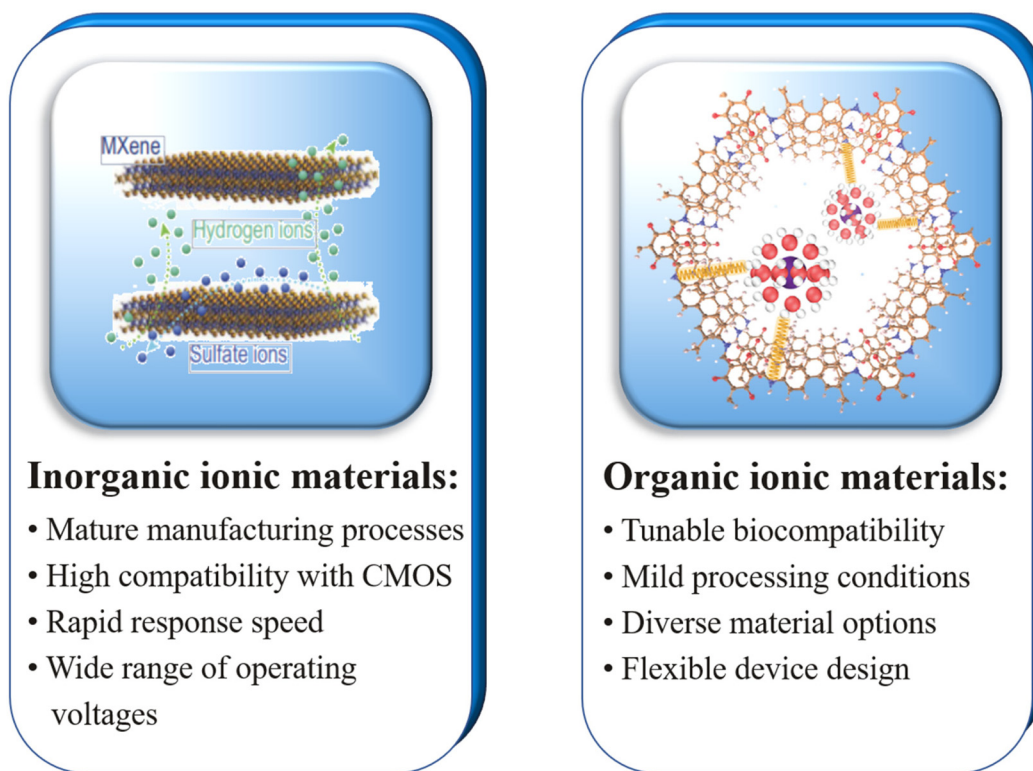


**Fig. 2** The performance comparison between inorganic ionic memristive materials and organic ionic memristive materials.<sup>71,72</sup> Reprinted with permission from ref. 71, © 2022 Oxford University Press; ref. 72, © 2021 Wiley.

Until now, a series of OIMs have been developed and yielded several distinctive advantages. For ionic small molecules, they usually exhibit good conductivity, enabling rapid response to external electrical signals and enhanced sensitivity. They also have high mechanical flexibility and plasticity, rendering them suitable for fabricating flexible electronic devices that afford extensive applications in smart watches, medical stickers and other fields.<sup>61,62</sup> Ionic polymers have excellent ion transport properties, which can realize data storage through ion migration and energy storage through ion conductance. Consequently, this kind of material finds wide applications not only in memristors but also in supercapacitors and battery energy storage systems.<sup>63,64</sup> Due to their exceptional chemical stability and precise control over ions, ionic liquids have also been extensively studied and applied in the fields of solar cells and flexible fuel cells, while they can also be prepared into thin films for metal protection, electronic device packaging, biomedicine, and so on.<sup>65–67</sup> In addition, OIMs can be applied in the domains of configurable circuits and multilevel memory, owing to their adjustable molecular structure, excellent optoelectronic properties, large specific surface area, controllable porosity, *etc.*<sup>68–70</sup> Overall, the unique characteristics of OIMs enable them to exert excellent performance and application in diverse fields, thereby manifesting their significance for further development and investigation in the future.

## 2.2. Specific categories of OIMs

OIM-based memristors typically exhibit ion transport characteristics, showing nonlinear resistance–current characteristics.<sup>73</sup> When a voltage bias is applied, the transport speed and direction of ions in OIM-based memristors will change, leading to a corresponding variation in the resistance value. According to the principle of memristors, the inherent nonlinearity performance enables memristive devices to efficiently store and process vast amounts of data, facilitating computation and logic operations based on ion transport. In addition, owing to the high diffusion velocity and low response time of the ion-active medium, OIM-based memristors hold immense potential for diverse applications encompassing artificial intelligence, neuromorphic computing, memory devices, and energy storage.<sup>32</sup>

Generally, OIMs can be divided into two categories, namely, ionically rigid conjugated materials (IICs) and ionically flexible spacer materials (IIFs).<sup>74</sup> IICs pertain to organic compounds featuring rigid conjugated molecular frameworks and cationic or anionic groups. Once an external electric field is applied, the IIC-based memristor will present resistive switching behavior. Considering the existence of rigid molecular frameworks, IICs usually exhibit high stability and a prolonged lifetime.<sup>74–76</sup> IIFs refer to organic materials with ions attached to flexible molecular chains. Under the application of an elec-

tric field, a reorganization of ions in the ionic liquid or colloid may lead to a modified resistance. Due to the presence of a flexible molecular framework, IIFs have a high ion transport speed and a fast response speed.<sup>77,78</sup> These two aforementioned categories of OIMs have broad application potential in the fields of energy storage, information storage, and sensing. However, it is imperative to meticulously select the appropriate material category according to the specific application requisites.

To give a more refined classification, OIMs can be divided into organic ionic small molecules and polymers, including ionic liquids,<sup>79–81</sup> polymeric ionic liquids,<sup>82</sup> ionic gels,<sup>160</sup> ionic conducting polymers,<sup>83–86</sup> coordination compounds (e.g., metal–organic frameworks (MOFs)),<sup>87–89</sup> some specific complexes, and so on.<sup>84,90–93,161</sup> All of these categories are introduced as follows (Fig. 3). (a) Ionic liquids can be designed and synthesized with varying compositions of ion pairs. They normally possess the advantages of low melting point, wide chemical resistance window, excellent ion transport properties, high adjustability, good thermal stability, and low volatility. Due to the relatively straightforward design and preparation process, ionic liquids with low fabrication costs can be easily synthesized on a large scale with a controllable size.<sup>79–81</sup> (b) Polyionic liquids are composed of ionic groups attached to polymer chains. In comparison with ionic liquids, polyionic

liquids exhibit enhanced stability and plasticity. Besides, they exhibit exceptional ionic conductivity, rapid ion transport velocity and reduced energy consumption. Polyionic liquids also demonstrate relatively high electrochemical stability and thermal stability.<sup>82</sup> (c) Ionic gels utilize organic gels containing ionic liquids as the active layer. The ionic liquid components provide high ionic conductivity, while the gel network offers mechanical stability and flexibility. At the applied voltage, the migration of cations and anions within the ionic gel enables resistive switching. The crosslinked gel structure helps maintain the ion distribution after removing the voltage. The integration of high conductivity and shape retainability makes ionic gels suitable for high-performance memristive devices. Ionic gels combine the dynamics of ionic liquids and robustness of gels, exhibiting both fast ion transport capability and form stability.<sup>160</sup> (d) Besides polyionic liquids and gels, other ion-conducting polymers are widely used in iontronic memristors. These ion-conducting polymers enhance ion transport properties by incorporating ionic groups into their molecular structures. They possess remarkable tunability and flexibility, where their electrochemical characteristics can be tuned by chemical modification. In addition, this kind of polymer generally exhibits exceptional conductivity and good durability.<sup>83–86</sup> (e) Ionic coordination compounds represent a category of structures wherein metal atoms and organic

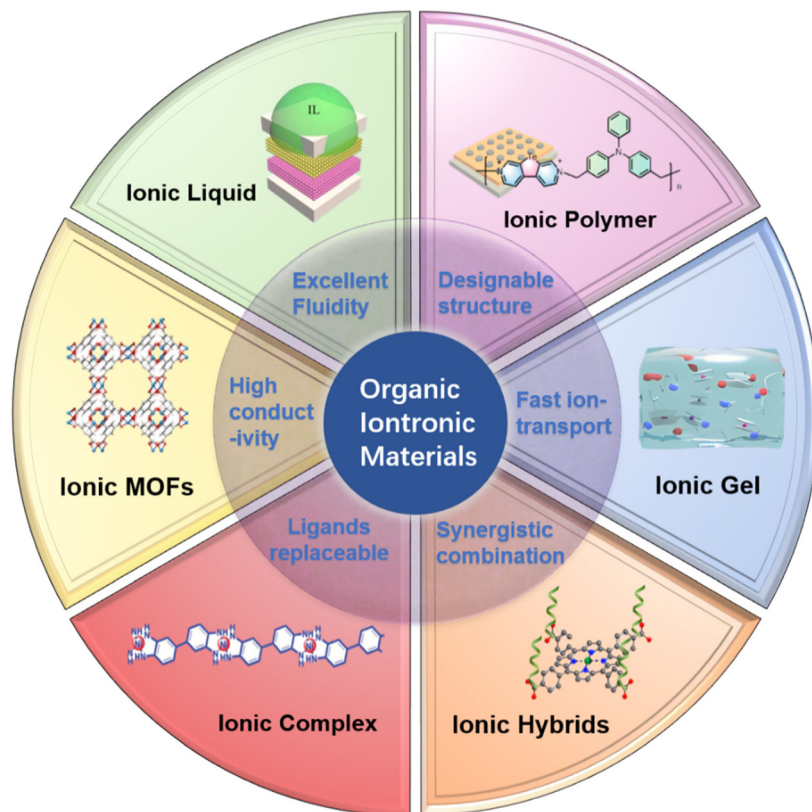


**Fig. 3** Different types of ionic memristive materials.<sup>93,95–97,160,161</sup> Reprinted with permission from ref. 93, © 2017 Wiley; ref. 95, © 2023 Wiley; ref. 96, © 2021 American Chemical Society; ref. 97, © 2021 Open Access; ref. 160, © 2023 Open Access; and ref. 161, © 2023 American Chemical Society.



ligands are linked by coordinate bonds. As a representative, MOFs show unique properties of high tunability, porosity and large surface areas. These materials can offer precise control over ion transport channels in iontronic memristors, while facilitating the storage and release of various ions within the material. Additionally, MOFs have superior thermal and chemical stability, along with remarkable scalability.<sup>87–89</sup> (f) Organic complexes exhibit both electronic and ion conductivity, serving as active layers in memristive devices. Under the stimulus of voltage, the resistive state of memristors can be modulated by the migration of ions in and out of the active layer. The unique electrochemical properties inherent to organic complexes make them attractive for utilization in memristors, resulting in low-power and energy-efficient operation.<sup>84,90–93</sup> Conclusively, ionic liquids and polyionic liquids have the advantages of low cost, easy preparation, high stability and plasticity. Other ion-conducting polymers, ionic coordination compounds and complexes exhibit the benefits of high tunability, excellent ion transport properties and good stability. All of these materials can cater to diverse application requirements including memristors.<sup>94</sup>

### 2.3. Preparation methods

To achieve these OIMs, various synthesis methods have been developed, including the ion exchange method, free radical polymerization method, solvothermal method and self-assembly method. (1) For the ion exchange method, the ion exchange reactions are performed between organic ligands and ions to form organic ionic materials,<sup>98</sup> which are suitable for the synthesis of organic ionic materials with specific structures and functions at high selectivity and a fast reaction rate. For instance, cation exchange resin is one of the most commonly used organic ion materials, due to its excellent ion exchange capacity and chemical stability.<sup>99</sup> However, it has limited regularity in terms of methodological procedures and preparation diversity, restricting its applicability to the preparation of specific types of ions.<sup>100</sup> (2) Free radical polymerization involves the polymerization of monomers containing ionic groups, resulting in the formation of ionic polymer materials with desired properties.<sup>101</sup> The key to this method lies in conducting monomer polymerization reactions using catalysts to form organic ionic polymer materials.<sup>102</sup> During atom transfer radical polymerization (ATRP), transition metal catalysts and upstream radicals can realize high selectivity and controllable polymerizations, offering predictable and diverse chemical structures.<sup>103</sup> (3) The solvothermal method needs the elevated temperature and pressure conditions of organic solvents to facilitate the formation of OIMs through dissolution and recrystallization.<sup>104</sup> This technique is particularly suitable for synthesizing OIMs with high crystal quality and uniform distribution.<sup>105</sup> Notably, solvothermal synthesis is employed to produce organic perovskite materials by the solvothermal method,<sup>106</sup> showing the high photoelectric conversion efficiency of solar cells and LED performances.<sup>107</sup> (4) The process of self-assembly involves the spontaneous arrangement of organic molecules into specific structures through

intermolecular interaction.<sup>108</sup> By selecting suitable organic ligands and the corresponding metal ions, organic ionic materials with specific morphologies and structures can be readily formed for various applications, such as liquid crystal displays, optoelectronic devices and sensors.<sup>109,110</sup> Overall, the ongoing research efforts in developing OIMs are expected to discover more novel synthetic methodologies that improve the properties and performance of OIMs for various electronic applications.

## 3. Memristive switching mechanisms

Unlike traditional electronic components, OIM-based memristors demonstrate a different operational mechanism. The memristive effect in OIM-based memristors depends on the quantity of charge and ions, holding promise to mimic human memory functions.<sup>111,112</sup> Specifically, when current flows through the memristor, the corresponding resistance may change as the increased applied voltage. If the resistance state of the device can be well maintained even after the removal of voltage, this device demonstrates typical nonvolatile memory behaviors.<sup>113</sup> Until now, some mechanisms have been promoted, including conductive filament formation,<sup>114–118</sup> charge trapping modulation,<sup>119–122</sup> *etc.*

### 3.1. Formation of conductive filaments

The formation of conductive filaments in memristors is attributed to the oxidation of active metal ions (*e.g.* Cu and Ag) into cations under an electric field, which migrate toward the cathode and are reduced back into metals, forming conductive paths between the electrodes and decreasing resistance.<sup>114</sup> After power removal, the instability of such paths causes the rupture and recovery of the high resistance state.<sup>115</sup> The formation and dissolution of conductive filaments can be modulated by the magnitude and polarity of the applied voltage. Recently, Sun *et al.* reported a memristor with a Ag/IGZO–TiO<sub>2</sub>/Al structure whose switching mechanism can be tuned by ionic liquids.<sup>96</sup> As illustrated in Fig. 4a, the operating principle of this device was elucidated through the following steps: (1) upon positive bias, metal ions (Ag<sup>+</sup>, Vo<sup>2+</sup>, H<sup>+</sup>) drift toward the cathode while O<sup>2–</sup> and e<sup>–</sup> move to the anode. (2) When Ag<sup>+</sup> is reduced into Ag atoms and connected with Vo<sup>2+</sup>, a conductive filament forms around the cathode. (3) Under reversed bias, opposite cations migrate back to the anode and anions back to the cathode. (4) As the reverse bias further increases, gradual rupture of the filamentary path occurs, recovering the high-resistance state.

In addition, ion migration is a critical mechanism governing resistive switching in memristors, participating in the formation and rupture of conductive filaments.<sup>116</sup> External stimuli such as light, electricity, heat, or chemical effects can induce the migration of ions, leading to the formation of conductive channels or non-conductive barriers and the corresponding switching of memristor resistance. Therefore, precise control of ion migration is crucial for the design of memristors

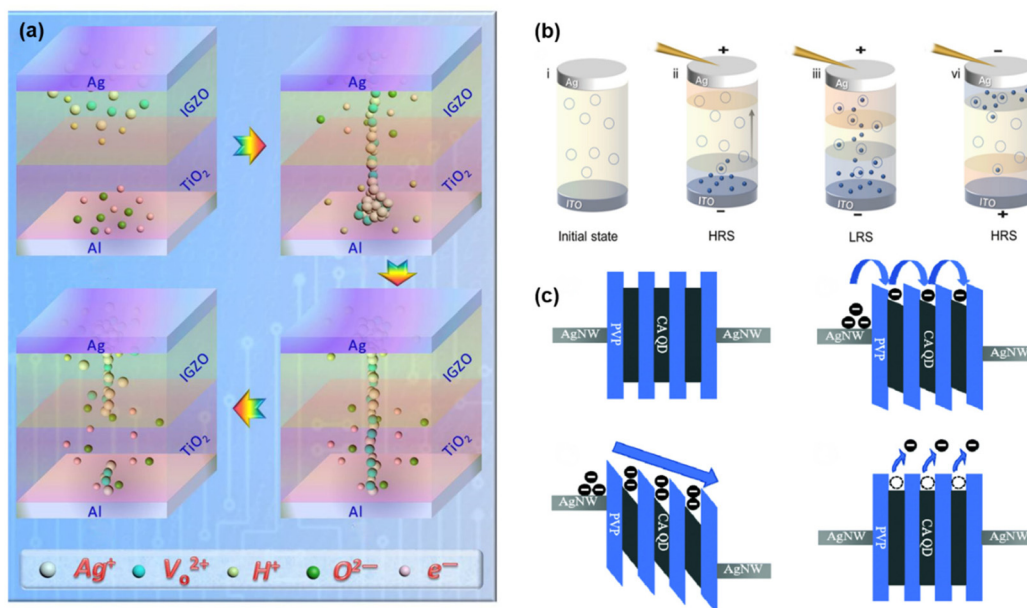


**Fig. 4** (a) Schematic illustration of the formation of conductive filaments.<sup>96</sup> (b) Model of the resistive switching mechanism.<sup>118</sup> (c) Schematic band diagrams to explain the resistive switching model.<sup>122</sup> Reprinted with permission from ref. 96, © 2021 American Chemical Society; ref. 118, © 2022 Science China Press and Springer; ref. 122, © 2018 Royal Society of Chemistry.

with desired performance.<sup>117</sup> Zhang *et al.* reported an ultrathin bio-memristor based on silk nanofiber films and analyzed its resistive switching behavior.<sup>118</sup> As depicted in Fig. 4b, multiple traps associated with sodium ions (Na<sup>+</sup>) exist in the nanofiber layer. When a positive voltage is applied on the top electrode, electrons migrate from the bottom electrode while cations in the layer move toward the negatively biased bottom electrode. An electric double layer (EDL) enriched with Na<sup>+</sup> forms at the interface, facilitating carrier trapping and migration. As the voltage further increases, instant saturated trap-filling leads to redundant carriers forming a conductive channel, inducing an abrupt transition from the high-resistance state (HRS) to the low-resistance state (LRS). The memristor recovers to the HRS when an opposite voltage is applied, releasing the trapped electrons toward the bottom electrode.

### 3.2. Modulation of charge trapping

The charge trapping mechanism refers to the process of modulating the trapping and release of charge carriers in the memristive layer.<sup>119</sup> Some certain carriers become trapped in defects or impurities in the insulating layer, leading to reduced resistance of the memristor.<sup>120</sup> Conversely, when a reverse bias is applied, the trapped charge carriers are released from their confinement, resulting in an increased resistance of the memristor. This charge-trapping modulation serves as a fundamental mechanism for the operation of specific types of memristors such as organic and amorphous oxide variants.<sup>121</sup> Zhou *et al.* employed a full solution process to prepare an Ag nanowire/citric acid quantum dot-PVA/Ag nanowire structure volatile memory device, and proposed a resistance switching mechanism model for memory devices.<sup>122</sup> As shown in Fig. 4c,

the thermally excited carriers dominate the conduction at a low bias voltage (0–0.7 V), wherein the device shows a high-resistance state. At a medium bias voltage (0.7–1 V), the injected carriers are dominant through trap-controlled space charge-limited mechanisms, which fall within the secondary region. When all traps are fully saturated, the injected carriers can move freely, leading to a sharp transition of the device into a low-resistance state. Upon removal of the bias voltage, the shallow traps fail to trap carriers, causing the device to revert back to a high-resistance state. The model elucidates the formation and destruction process of the conductive path in the dielectric layer driven under an external electric field, and explains the reversible resistance-switching behaviors.

### 3.3. Redox mechanism

Redox reactions serve as a significant mechanism for resistive switching in certain types of memristors. The active layer in these devices typically contains electrochemically active species that can undergo oxidation or reduction when subjected to an electric field.<sup>151</sup> For example, in electrochemical metallization cells with a solid electrolyte, metal ions such as Cu<sup>2+</sup> and Ag<sup>+</sup> can be reduced at the cathode, leading to the formation of conductive metallic filaments that bridge the electrodes.<sup>152</sup> Reversing the voltage bias will result in the oxidation and dissolution of these filaments, thereby increasing the resistance of the device.<sup>153</sup>

In organic memristors, the redox-active groups embedded in the organic matrix play a crucial role in modulating charge transport and resistance states, which have been observed in certain types of memristive devices. These redox-active groups, such as nitro and acene, undergo reversible oxidation/

reduction reactions when subjected to external voltage. During these redox reactions, ion migration occurs as counterions need to balance the charges generated by the oxidation or reduction processes. The movement of ions within the organic matrix further influences the overall resistance state of the memristor.<sup>154</sup> To develop high-performance memristors, it is essential to have precise control over these redox processes. Understanding the reaction kinetics involved and studying ion migration dynamics can greatly contribute to optimizing the memristor performance, including device stability, switching speed, and increasing endurance.<sup>155</sup> Therefore, this knowledge will pave the way for advancements in memristor technology that could revolutionize various fields including data storage, neuromorphic computing systems, and flexible electronics.

## 4. OIM-based memristor applications

OIM-based memristors utilize both the semiconductor characteristics and ionic transport properties during the device operation. Active media encompass various substances, such as small molecules, complexes, ionic liquids, ion-conducting polymers and polymeric ionic liquids.<sup>81,82,91,93,123,124</sup> In the context of memristive devices, the resistive states can be modulated by the migration of ions in and out of the active layer under an externally applied electric field.<sup>32,125</sup> The potential of these devices in low-cost and flexible electronics, as well as their ability to exhibit analog behavior, has garnered significant attention (Table 1). Therefore, developing high-performance OIMs is crucial to advancing the field of organic iontronic memristors and realizing their potential in a range of electronic applications.<sup>43</sup>

### 4.1. Small molecule OIM-based memristors

Small molecule OIM-based memristors utilize organic small molecule OIMs as the data-storage medium, where the migration of ions or electrons is controlled to adjust their resistance/conductance. Typically, ions or electrons can migrate within the active layer at an applied voltage. Different ion or electron migration behaviors result in varying resistance altera-

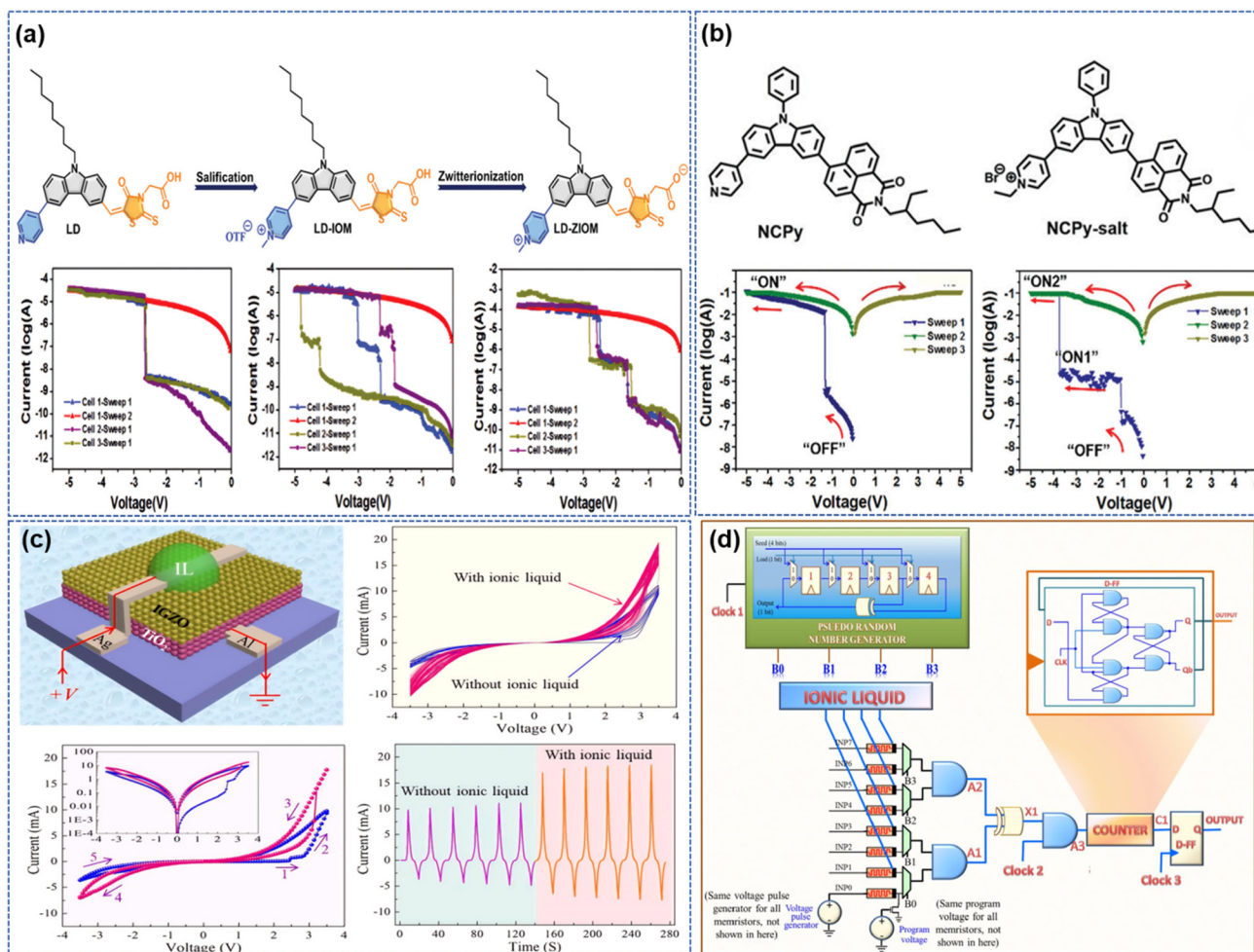
tions, leading to information storage and reading operations. Unlike inorganic materials with well-defined crystalline properties, organic materials often present isotropic molecular orientations and diverse organizational forms, giving rise to unpredictable morphologies and device performance. Commonly, the performance of organic small molecule memristors could be enhanced by modifying the chemical structure of the active layer. For example, Zhang *et al.* synthesized two fresh ionic and zwitterionic donor/acceptor (D/A) conjugated small molecules (LD-IOM and LD-ZIOM).<sup>126</sup> Compared to neutral parent structures, these two newly-synthesized ionic and zwitterionic D/A conjugated small molecules show improved optoelectronic performances (Fig. 5a). In addition, Zhang *et al.* also synthesized a new pyridine-based organic conjugated molecule (NCPy) and converted it into an organic pyridinium salt (NCPy-salt).<sup>73</sup> The transition from NCPy to ionic NCPy salts produced highly oriented nanofibers and high-quality films. The NCPy salt-based devices undergo two “writing” processes, transitioning from the OFF state to the medium conductivity (ON1) state and further to the high conductivity (ON2) state. The device exhibits a current switching ratio of  $10^6/10^2/1$ . Owing to the salification, a unique ternary resistive switching memory behavior was observed, implying potential applications in high-density data storage and memory (Fig. 5b). The stability and repeatability of the small molecule memristor were fully confirmed through measurements conducted on over 50 device units, as well as a persistence test lasting more than 5000 s.

The inclusion of small molecule ionic liquid materials has expanded the selection range of memristive materials. Ionic liquids have high ionic conductivity, resulting in reduced threshold voltage and low power consumption for these memristors. To increase the storage density, Sun *et al.* used an indium gallium zinc oxide (IGZO)-TiO<sub>2</sub> bilayer film as the functional layer within the memristive device (Fig. 5c).<sup>96</sup> By utilizing diethylmethyl(2-methoxyethyl)ammonium bis(trifluoromethylsulfonyl)imide (DEME-TFSI), an ionic liquid known for its flexibility, it was able to fine-tune the memory behavior of the device. The device exhibits excellent switching stability and retention, with the HRS and the LRS lasting for a minimum of

**Table 1** The summary of the performance of different OIM-based devices

Materials	Category	Current ratio	Other features	Ref.
NCPy	Small molecule	$10^3$	—	73
NCPy-salt	Small molecule	$10^6/10^2$	Retention time $> 5 \times 10^3$ s	73
DEME-TFSI	Small molecule	—	Retention time $> 10^5$ s	96
SA-Bu	Zwitterionic	$10^5/10^2$	Retention time $> 10^4$ s Response time 190 s (NO <sub>2</sub> )	128
CA-Bu	Zwitterionic	$10^7$	Retention time $> 10^4$ s	128
PTeVTPA	Polymer	—	High-pass filter	97
Ni-BTA	Complex	$10^7/10^3$	Retention time $> 10^4$ s	93
Ni-BPTA	Complex	$10^8/10^4$	Retention time $> 10^4$ s	93
Au-NPs	MOFs	$10^4$	High stability $> 200$ times	87
Ag-NPs	MOFs	$10^3$	High stability $> 200$ times	87
SNFs	Bio-nanofibrils	$10^2$	Retention time $> 10^5$ s High stability $> 180$ times	118







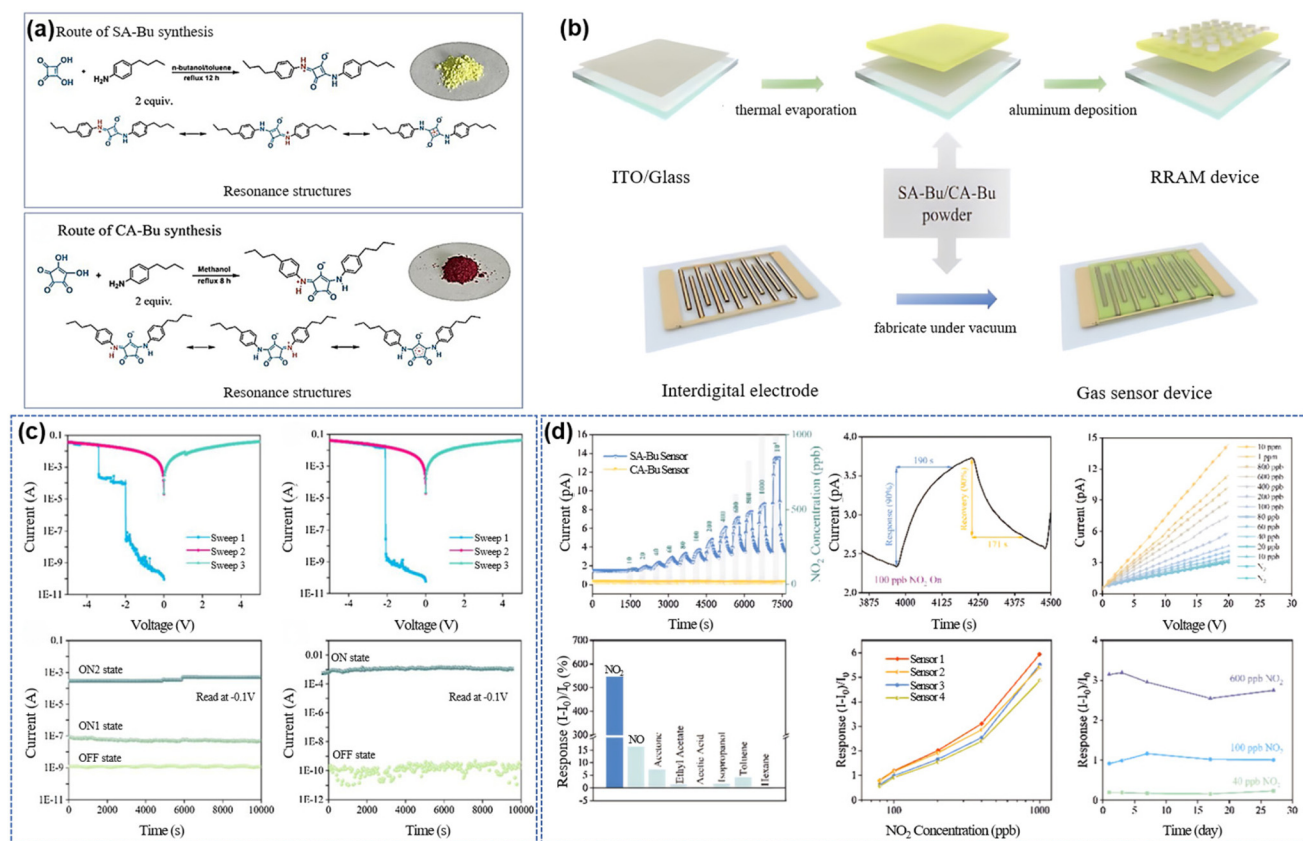


**Fig. 6** (a) Synthetic routes of SA-Bu, CA-Bu and their zwitterionic resonance structures. (b) Schematic diagram of fabricating RRAM and gas sensor devices. (c) Typical tri-state  $I-V$  and stability test characteristics of SA-Bu/CA-Bu based memory devices. (d) Transient response of SA-Bu and CA-Bu sensors with an increase in  $\text{NO}_2$  concentration.<sup>128</sup> Reprinted with permission from ref. 128, © 2021 Elsevier.

statistical analysis was performed on 120 samples, revealing an approximate device yield of 41% for the three-component system. Consequently, SA-Bu is able to realize three different resistance states in the memory device cell, giving it more capacity and flexibility for information storage. For CA-Bu, due to the steric distortion of a conjugated structure, it exhibits a binary memory behavior with reduced conductivity and responsiveness to  $\text{NO}_2$ . The implication here is that the establishment and regulation of the conjugated structure play a pivotal role in attaining optimal electrical conductivity and memory performance when designing organic zwitterionic memristors.

Wang *et al.* adopted commercially available organic dyes, Rhodamine B and Rhodamine 6G, as active materials for low-cost, easy-to-manufacture multilevel RRAM devices.<sup>123</sup> The as-fabricated RRAM exhibits a ternary write-once-read-many (WORM) type memory behavior with a retention time of up to 5000 s. Due to the strong intermolecular interactions between the dye molecules, these rhodamine-based memristors can work stably at temperatures up to 80 °C. Furthermore, they demonstrate that the flexible RRAMs can be fabricated on different substrates, such as polyethylene terephthalate (PET), postage stamps and leaves, while maintaining their retention even after being bent more than a thousand times. The

research in the field of zwitterionic memristors is still in its nascent stage, yet it has exhibited promising device performance and functionality. The ongoing advancement of novel materials incorporating amphoteric ions, along with the optimization of the device architecture and manufacturing techniques, is in urgent need.

#### 4.3. Polymer OIM-based memristors

Organic polymer memristors generally adopted D/A conjugated polymers as the active layer. These kinds of devices can operate by modulating the charge transport properties of the polymer under an external electric field, resulting in resistance changes and non-volatile memory behavior. Organic polymer memristors often exhibit high switching speeds and large on/off ratios, making them highly attractive for applications in high-speed memory and neuromorphic computing. In the field of organic polymer memristors, researchers are striving to improve the performance and stability of these devices. Through optimization of the geometric construction, ratio and synthesis method of the polymer, superior electrical conductivity and memristive properties have been achieved. As shown in Fig. 7a and b, Zhao *et al.* successfully designed and synthesized a series of D/A conjugated polymer PCVTPA by directly coupling cation-anion V-TPA units containing sulfur

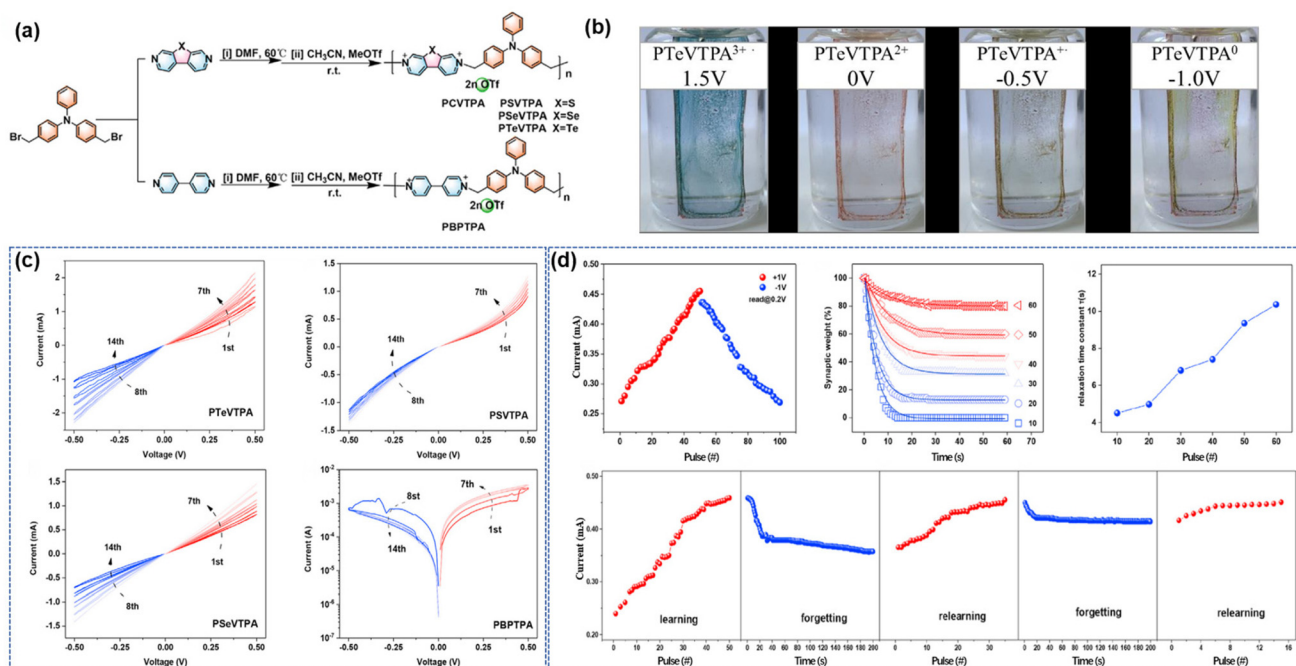


**Fig. 7** (a) Synthesis of PCVTTPA (PSVTTPA, PSeVTTPA, PTeVTTPA) and PBPTTPA. (b) Electrochromic photographs of the PTeVTTPA thin film coated onto the ITO substrate. (c)  $I$ - $V$  characteristics of the Al/polymer/ITO devices. (d) Synaptic function simulation in human brain memory behavior, including repetitive learning forgetting (STP/STD).<sup>97</sup> Reprinted with permission from ref. 97 © 2021 Open Access.

(PSVTTPA), selenium (PSeVTTPA) and tellurium (PTeVTTPA).<sup>97</sup> The sandwich structure device of Al/PCVTTPA/ITO showed a typical memristive effect. By incorporating S, Se and Te into the V-TTPA unit, the device demonstrated superior performance. The process of simulating the “learning, forgetting, and re-learning” of the human brain is achieved by applying continuous pulses. The third time it reaches the same learning level only requires 15 pulses out of the first 50 continuous pulses, while simultaneously exhibiting a significantly slower rate of forgetting compared to the second time (Fig. 7c and d). This study achieves the integration of high-performance synaptic simulation and brain-like computing functions within a single electronic device, presenting a novel approach to build intelligent computing systems. The research demonstrates the significant potential of this material in constructing artificial neural networks for neuromorphic computing and intelligent computing systems, which is capable of performing arithmetic operations on decimal numbers.

Wang *et al.* combined a MXene/thermoplastic polyurethane (TPU) tensile sensor to construct an Ag ionic polymer-metal composite (IPMC) actuator, a new flexible threshold switch (TS) device for an unconditional reflective arc system.<sup>124</sup> By utilizing the internal silver nanowire (NW) channel, the system can be adjusted according to varying operating conditions, which can effectively emulate a fundamental reflection arc and enable basic self-control capabilities. NW-based memristors exhibit significant potential for various applications, because of their simple preparation process, versatile modulation constraints and inherent self-recovery characteristics. The relative

resistance change rate reaches a remarkable value of 525.62 when the maximum effective stretching reaches 40%. Simultaneously, the actuator demonstrates its reversibility and reliability by withstanding 10 cycles of cyclic voltage switching from 3 to  $-3$  V. The field of polymer OIM-based memristors has witnessed significant advancements in recent years, with numerous studies highlighting exceptional device performance and stability.<sup>83</sup> However, challenges persist in terms of achieving prolonged stability and reproducibility. Continuous development of novel conjugated polymer OIMs, alongside the optimization of device architecture and processing techniques, is anticipated to propel this field forward.

#### 4.4. Complex OIM-based memristors

Organic complex memristors utilize an organic complex as the active layer, which is composed of central metal ions and organic ligands. The performance of memristors can be regulated by adjusting the properties of metal ions and ligands. Compared with traditional inorganic memristors, organic memristors have higher adjustability and controllability, offering multi-level resistance changes and fast switching speeds. Similar to organic small molecule memristors, organic complex memristors also possess the advantage of low power consumption, flexibility and ease of processing. For organic complexes, they have been extensively investigated to improve the device performance through the optimization of the coordination environment, complex structure and ligand selection. For example, diverse storage behaviors and performances can be achieved by conducting devices under various synthetic

conditions. Zhang *et al.* proposed a simple interfacial synthesis method and successfully prepared large-area 2D coordination polymer films.<sup>84</sup> The polymer film can be transferred to any independent substrate, providing the possibility to develop solution-processed non-volatile memory devices. The device exhibits a stable current of about 0.04 A at a constant voltage stress of 0.5 V, lasting up to  $10^4$  s, maintaining a high on/off current ratio of  $10^3$ , and precise control of the on and off states ensures the memory device's low misreading rate. This work demonstrates an innovative approach to designing memory devices based on 2D coordination polymer films through interface nanostructure engineering, and thus, proposing new ideas for the further development of non-volatile memory devices.

As shown in Fig. 8a and b, Cheng *et al.* reported the successful fabrication of ternary resistive random access memory (RRAM) devices using 1D  $\pi$ -d conjugated coordination polymer chains as the active layer.<sup>93</sup> The two polymers, Ni-BTA and Ni-BPTA, were synthesized *via* a solution-based method and exhibited good thermal stability, attributed to their robust intermolecular interactions. As shown in Fig. 8c and d, these materials demonstrate maximum switching current ratios as

high as  $10^7$  and  $10^8$ , and all three levels of both aged devices can last and read for more than  $10^4$  s after 100 days of storage. High temperature stability and long-term environmental durability make it very promising for next-generation data storage through RRAM technology. Besides, these materials also own potential applications in molecular-based ferromagnets, synthetic metal conductors, nonlinear optical materials, iron electricity, and other electronic fields. The significance of molecular structure tuning in the design of organic complex memristors is evident from these studies. Rational design and optimization of molecular structures can facilitate diverse storage behaviors and superior performance. Therefore, this work offers novel ideas and prospects for advancing high-performance and tunable properties in complex OIM-based memristors.

#### 4.5. Other OIM-based memristors

In addition to the aforementioned types of memristors, there are several other types of memristors that have been investigated in recent years. For instance, an organic composite memristor contains the interaction between the organic and inorganic components.<sup>129</sup> Zhao *et al.* reported the synthesis of

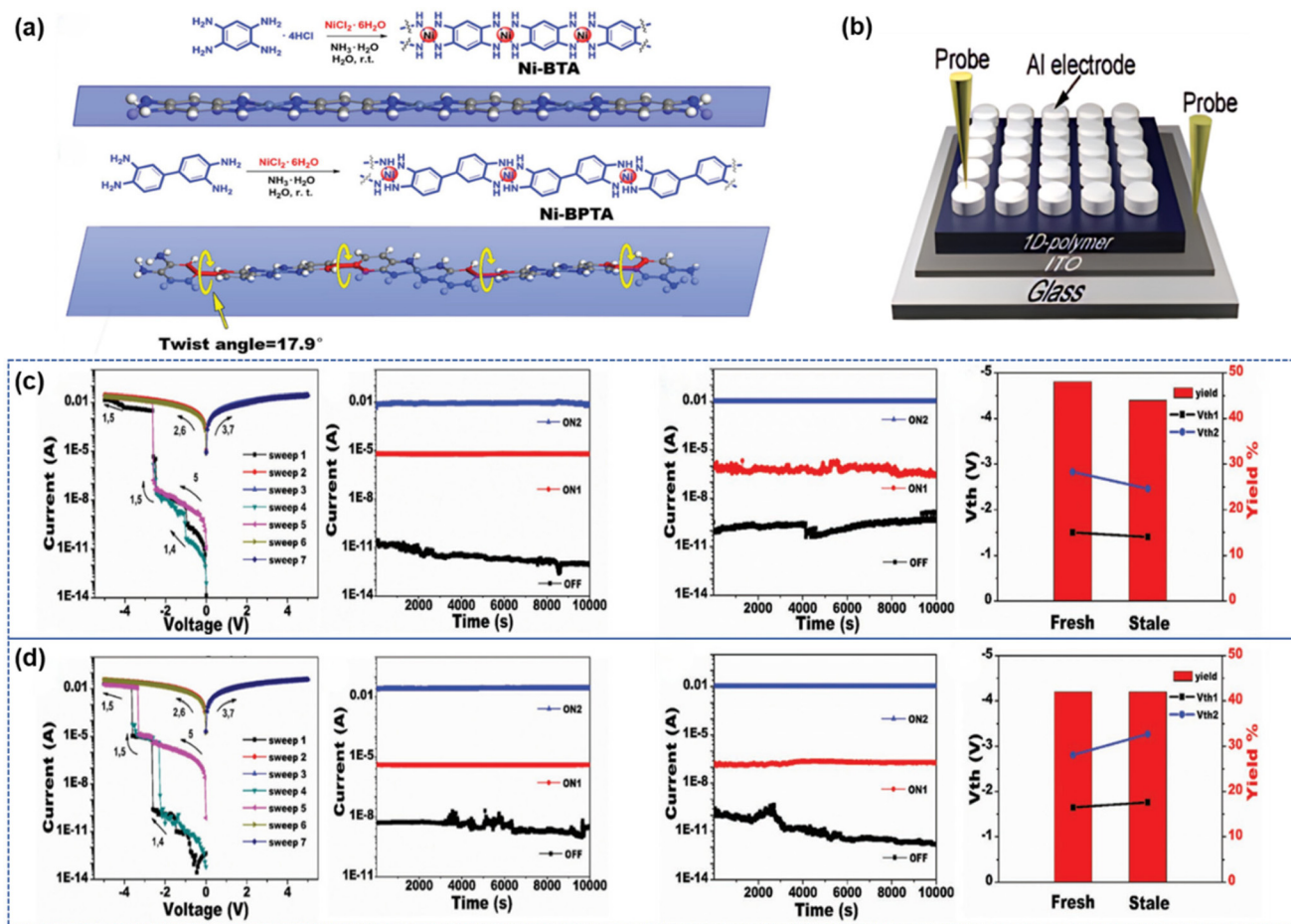


Fig. 8 (a) Synthetic routes and geometry of Ni-BTA and Ni-BPTA. (b) Typical sandwiched structure of memory devices. (c and d) Characteristic  $I$ - $V$  curves, stability, threshold voltage and ternary device yield of (c) Ni-BTA and (d) Ni-BPTA.<sup>93</sup> Reprinted with permission from ref. 93, © 2017 Wiley.



Au and Ag nanoparticles (NPs) embedded in 3D Cd-based MOF matrixes *via* a photoreduction method, producing Au (Ag)-NP@MOF composite materials.<sup>87</sup> Electrical bistability measurements on the sandwiched ITO/NP@MOF/Ag device showed two switchable conductivity states of the device with non-volatile memory behaviors. This was attributed to an electric-field-induced charge transfer process aided by conformational changes in the active layer. Among the tested samples, the ITO/Au NP@2/Ag device with a neutral MOF

matrix had the highest ON/OFF current ratio of  $10^4$ , owing to a better dispersion of Au NPs in the MOF matrix resulting in more efficient electron tunneling.

Another type is a bio-memristor, inspired by biological systems like synaptic connections between neurons in the brain.<sup>130–133</sup> Zhang *et al.* reported the fabrication of an ultra-thin bio-memristor based on silk nanofibrils (SNFs) (Fig. 9a). As shown in Fig. 9b–g, the SNF-based device showed a low operating voltage, good stability and environmental friendli-

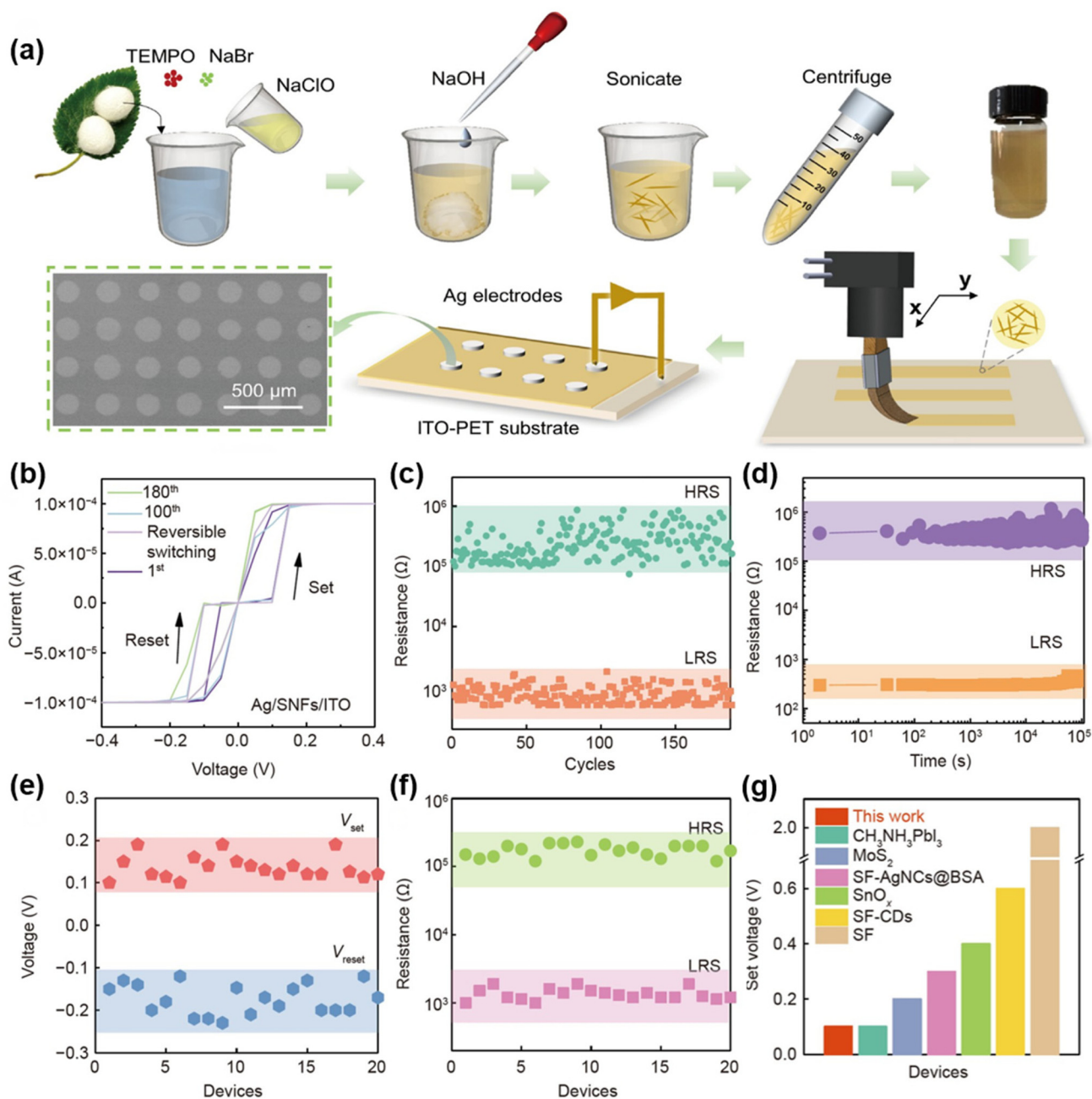


**Fig. 9** (a) Schematic diagram illustrating the preparation of the ultra-thin SNF-based memristor. (b) Typical  $I-V$  characteristics of the SNF-based memristor. (c) Endurance performance and (d) time retention measurements of the Ag/SNFs/ITO memristor. (e and f) The  $V_{set}$ ,  $V_{reset}$  and the resistance distributions of Ag/SNFs/ITO memristors. (g) Comparison of the set voltages for different memristors.<sup>118</sup> Reprinted with permission from ref. 118, © 2022 Science China Press and Springer.



ness.<sup>118</sup> Besides, the device demonstrated a high dielectric performance due to its intrinsic ionic conductivity and nanoscale thickness. As a result, the SNF-based memristor presented stable resistive switching over 180 cycles and a retention time of up to  $10^5$  s. The integration of SNF-based memristors into a crossbar array achieves consistent memristive performance for image memorization as well as logic operation functions. All of these types of memristors offer unique advantages and opportunities, prompting ongoing research efforts to develop novel materials and devices that can optimize their performance and facilitate new applications.

## 5. Extended applications

The unique properties of memristors, such as nonvolatile memory, low power consumption, and analog computing capabilities, have demonstrated significant potential in various device applications.<sup>134,135</sup> Specifically, OIM-based memristors offer distinct advantages in neural simulation, brain–computer interfaces and the efficient photoelectric effect, due to their utilization of ionic–electronic materials with exceptional properties.<sup>136–138</sup> Some distinct properties of OIM-based memristors should be noted. Firstly, OIM-based memristors have good biocompatibility and can be directly integrated into organisms, providing the possibility to build bioelectronic interfaces. The polymorphism properties of OIMs can complete different oxidation states, simulating the potential functionality of neurons and multi-level data-storage behavior, thereby facilitating the realization of a more realistic neural network. OIMs can be easily prepared by simple solution deposition or printing techniques, which hold promise to produce large-scale neural networks. By adjusting the chemical structure of OIMs, their electrical properties can be precisely regulated. Therefore, the electrophysiological parameters of various neurons can be customized. Additionally, some OIMs have strong photo-responsiveness, which can directly convert light signals into electrical signals, meaning that the highly sensitive optoelectronic neurons can be mimicked. Consequently, OIMs play a significant role in fabricating flexible devices, which is conducive to achieving wearable neuroelectronic applications.

The utilization of OIM-based memristive materials offers distinct advantages in the field of biomimetic electronics, facilitating efficient emulation of neural networks and interfaces for human–computer interaction.<sup>138</sup> Through fast switching and programmable conductivity states, these materials are able to mimic the excitatory and inhibitory states of neurons, enabling intricate computations within neural networks. In addition, its low power consumption and high stability render it highly suitable for the development of brain–computer interfaces.<sup>137</sup> By integrating with biocompatible materials, OIMs can effectively interact with the human brain and promote the advancement of brain–computer interface technology. Meanwhile, OIMs also exhibit a diverse range of photosensitive properties, which can achieve fast and reversible responses. Such characteristics will greatly actuate the advancement of

efficient light control devices and optical memory.<sup>136</sup> OIMs have broad application prospects in the fields of biomimetic electronics, intelligent computing and medical electronics.

### 5.1. Simulated biological synapse simulation

The importance of human brain synapses in memory and learning lies in their remarkably low power consumption and superior performance compared to supercomputers.<sup>60</sup> To develop suitable electronics for artificial neural networks (ANNs), the OIM-based device must demonstrate energy efficiency comparable to that of human brain synapses.<sup>139,140</sup> Synapse simulation is considered an important step toward efficient ANNs similar to the brain.<sup>141,142</sup> However, previous attempts to take advantage of complementary metal–oxide–semiconductor (CMOS) technology have resulted in increased energy consumption and complexity, posing challenges for high-density neural networks.<sup>143</sup> By contrast, Zhang *et al.* produced an artificial synapse based on flexible PET substrates, exhibiting unique history-dependent memory behaviors,<sup>86</sup> analogous to the synaptic enhancement and inhibition in neurobiology. The device also showed basic synaptic plasticity and some human memory and learning behaviors. Furthermore, the study showed that even with a bending radius of less than 10 mm, the device still showed a unique synaptic performance. This indicates the potential utilization of such devices in constructing wearable neuromorphic computing systems. In addition to mimicking neural pathways in the brain, OIMs are also used for simulating biological behaviors. Wang *et al.* presented an innovative artificial device to replicate the bladder relaxation reflex arc found in biological systems (Fig. 10a).<sup>124</sup> This device successfully converted continuous extension signals into control signals, adhering to the all-or-nothing principle. As shown in Fig. 10c and d, by combining an MXene/TPU tensile sensor, an Ag IPMC actuator and a new flexible threshold-switching device, they constructed an unconditional reflective arc system, with a 10%–40% strain range similar to bladder expansion and a maximum strain response up to 225%. As the bladder expands when filled with fluid, the sensor is stretched and modulates the memristor's resistance through parallel connection, triggering the actuator contraction upon reaching a threshold to simulate the bladder relaxation reflex. They proposed to use flexible materials with neuromorphological control in medical and intelligent robotics applications, while simulating unconditional reflexes through the utilization of threshold-switching memristors as sympathetic nerve centers.

### 5.2. High-density data storage

The utilization of OIMs in memristors presents numerous advantages in the realm of high-density data storage. These devices possess non-volatile memory properties, enabling them to retain the as-stored data for extended periods even during power outages.<sup>144</sup> This property exhibits enormous advantages in scenarios involving temporary power disruptions or interruptions. Owing to their operating mechanism based on ion transport or charge injection, organic iontronic

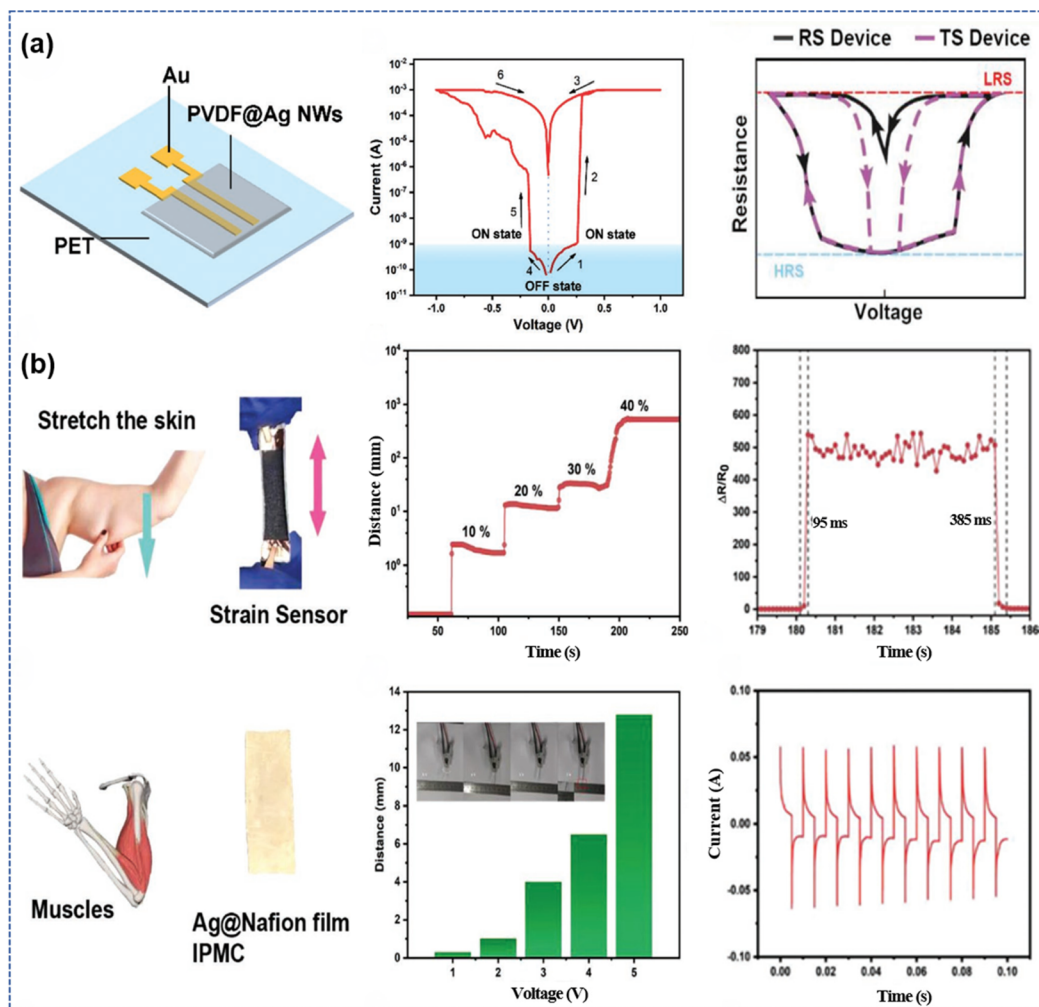


Fig. 10 (a) Statistical diagram of urine accumulation and excretion in the bladder and schematic representation of the resistance. (b) The bladder diastolic reflex and corresponding electrical tests.<sup>124</sup> Reprinted with permission from ref. 124, © 2022 Wiley.

memristors can achieve higher information densities compared to conventional memory technology.<sup>145,146</sup> Therefore, OIM-based memristor holds high promise for large-scale high-density data storage. Sun *et al.* designed an IGZO-based memristor regulated by DEME-TFSI ionic liquids. A memristor array was integrated to produce a true random number generator for secure communication or radar waveform design, *etc.*<sup>96</sup> They found that such devices could be applied not only for data storage, but also opened up potential applications in cryptography. Besides, this device showed high packing density and excellent compatibility with the existing CMOS processes. Therefore, this work paves the way for advancing nanoscale technologies that can potentially supplant current CMOS technologies. In addition, OIM-based memristors also favor achieving high-frequency writing/reading speeds and low power consumption. Wang *et al.* successfully fabricated cost-effective and easily manufacturable multilevel RRAM using commercially available dyes Rhodamine B and Rhodamine 6G.<sup>123</sup> The as-fabricated RRAM exhibited ternary WORM-type

memory behaviors, which could be attributed to the strong intermolecular interactions between the dye molecules. These rhodamine-based reservoirs could even work stably at temperatures up to 80 °C.

### 5.3. Integrated photovoltaic memristors

The application of memristors in optoelectronic devices also presents broad prospects. By combining memristors with optoelectronic elements, it becomes feasible to realize memristor-based optoelectronic memory devices for controlling and storing optical properties.<sup>147</sup> Simultaneously, memristors can also be used to achieve photoelectric conversion devices, thereby converting light energy into electrical energy or *vice versa*. By introducing light-absorbing materials into the device, OIM-based memristors can realize efficient photoelectric conversion. These applications will play a vital role in the fields of photoelectric information, photoelectric sensing and detection, and photoelectric devices, offering vast development potential.<sup>148</sup>

Yang *et al.* carried out the development of photovoltaic memristors based on bulk photovoltaic effect (BPVE) devices with similar synaptic plasticity to biological synapses.<sup>127</sup> The photovoltaic synaptic plasticity in BPVE devices is closely associated with the dynamics of domain switching in ferroelectric thin films. This device demonstrates highly discernible changes in the photovoltaic response that can be continuously adjusted from low to high levels. Additionally, spike timing-related plasticity (STRP) can be harnessed through the diverse modes of domain switching dynamics of double pulses. Photovoltaic memristors employ optical reading instead of high-frequency electrical reading, thereby increasing the reading speed and reducing the energy consumption.

## 6. Conclusions and perspective

In summary, OIMs and their memristors, as a novel category of memristive materials and devices, have received increasing attention due to their advantages such as a high switching ratio, low power consumption, substantial switching durability, and compatibility with flexible substrates.<sup>149</sup> Over the past decade, they have been extensively investigated. These newly-designed materials and their doped complexes have significantly enhanced device performance, making them suitable for various applications, including neuromorphic computing, artificial intelligence, energy storage, and so on.<sup>150</sup> In this review, we introduced the basic concept and synthetic methods of OIMs, and discussed the various applications of OIM-based memristors. Their advantages relative to other memristors were also highlighted. The different types of OIMs possess different transmission speeds, power consumption, storage capacities, *etc.* Therefore, the functionality of organic iontronic memristors can be determined by a comprehensive analysis. The topics covered in this section encompass ion transport kinetics and some other typical memory mechanisms. For OIMs, the kinetics of ion transport is a core factor influencing the performance of iontronic devices, including response speed, power consumption and stability of the devices. The modulation strategies of ion transport kinetics involve the design and optimization of the device structure, materials selection, device interface engineering, *etc.*, which can be used to improve the efficiency and controllability of ion transport. Therefore, an in-depth understanding and control of ion transport kinetics will provide important guidance for the development of ion electronics. By exploring new materials, interface engineering, and optimizing device structures, it is expected to further improve the efficiency and controllability of ion transport properties, bringing more opportunities for the application fields of ion electronics.

Although significant progress has been achieved in the development of OIMs as well as their memristors, some challenges still remain to be addressed in the future. Firstly, the switching speed and response time of OIM-based memristors need to be further improved through interface engineering and nanostructure optimization to meet the demands of high-

speed information processing and transmission. For example, novel electrode materials and device architectures could be explored to lower the energy barriers for ion migration. Secondly, the durability and cyclability of OIM-based devices should be enhanced by improving material stability and conducting appropriate encapsulation. The device lifespan could be extended by inhibiting the side reactions between the active layer and electrodes. Developing OIMs with high thermal/chemical stability is also vital. Thirdly, new electrode materials such as graphene, carbon nanotubes and conductive polymers could be explored to improve the charge injection efficiency at the electrode/OIM interface. Appropriate electrode selection and surface modification are keys to achieving ohmic contacts. Fourthly, more theoretical and experimental efforts are still needed to reveal the detailed ion transport mechanisms and kinetics in OIMs. Advanced characterization techniques, such as conductive atomic force microscopy, could provide valuable insights. Molecular dynamics simulations may help understand the ion conduction processes. Fifthly, the integration and compatibility of OIM-based memristors with CMOS circuits remain a challenge. Innovative device fabrication processes and creative circuit designs are required to address this integration issue. Finally, new OIMs with superior comprehensive performances, including high speed, large ON/OFF ratio, long endurance, and excellent stability, need to be developed through molecular design, synthesis and nanoengineering. Systematic material optimization is the key to achieving ideal OIMs.<sup>156,157</sup> We believe that with continuous research efforts, the challenges faced by OIM-based memristive devices could be gradually conquered, unleashing their application potential in next-generation electronics.

Overall, OIM-based memristors have demonstrated great potential in various applications, such as data storage, artificial intelligence, neuromorphic computing, energy storage, sensors and other fields.<sup>158,159</sup> We believe that the challenges discussed here can be effectively solved through collaborative efforts. Future work on OIMs will undoubtedly continue to pave the way for further development of memristive devices, and we remain optimistic regarding the applications of these devices in the forthcoming years. With the advancement of technology and the expansion of prospects, iontronic memristors will play a significant role in the future intelligent electronic field.

## Author contributions

The manuscript was written through contributions of all authors. All authors have given approval to the final version of the manuscript.

## Conflicts of interest

The authors declare no competing financial interest.

## Acknowledgements

Y. L. acknowledges financial support from the National Natural Science Foundation of China (Grants No. 22008164 and 62304148), the Natural Science Foundation of Jiangsu Province (Grants No. BK20230074), the Youth Talent Support Program of Jiangsu Association for Science and Technology (TJ-2023-033), the Youth Talent Support Program of Suzhou Association for Science and Technology (2023-04), the Natural Science Foundation of the Jiangsu Higher Education Institutions of China (Grants No. 22KJB150037), and the Foundation of Key Laboratory of Synthetic and Biological Colloids, Ministry of Education, Jiangnan University (No. 1042050205225990/007). This work is also supported by the Postgraduate Research & Practice Innovation Program of Jiangsu Province (KYCX23\_3304), Jiangsu Key Disciplines of the Fourteenth Five-Year Plan (2021135), and the Suzhou Key Laboratory for Low Dimensional Optoelectronic Materials and Devices (SZS201611), and Research in Cutting-Edge Technology of Suzhou (SYG202351).

## References

- D. Feng, Z. Niu, J. Yang, W. Xu, S. Liu, X. Mao and X. Li, *Nano Energy*, 2021, **90**, 106526.
- A. M. Ionescu and H. Riel, *Nature*, 2011, **479**, 329–337.
- X. Zhao, Z. Wang, Y. Xie, H. Xu, J. Zhu, X. Zhang, W. Liu, G. Yang, J. Ma and Y. Liu, *Small*, 2018, **14**, 1801325.
- J. B. Roldan, E. Miranda, D. Maldonado, A. N. Mikhaylov, N. V. Agudov, A. A. Dubkov, M. N. Koryazhkina, M. B. Gonzalez, M. A. Villena, S. Poblador, M. Saludes-Tapia, R. Picos, F. Jimenez-Molinos, S. G. Stavrinos, E. Salvador, F. J. Alonso, F. Campabadal, B. Spagnolo, M. Lanza and L. O. Chua, *Adv. Intell. Syst.*, 2023, **5**, 6.
- F. Zahoor, T. Z. Azni Zulkifli and F. A. Khanday, *Nanoscale Res. Lett.*, 2020, **15**, 90.
- Y. Ren, C.-L. Chang, L.-Y. Ting, L. Zhou, J.-Y. Mao, S.-R. Zhang, H.-H. Chou, J.-Q. Yang, Y. Zhou and S.-T. Han, *Adv. Intell. Syst.*, 2019, **1**, 1900008.
- N. Raeis-Hosseini, Y. Park and J.-S. Lee, *Adv. Funct. Mater.*, 2018, **28**, 1800553.
- Y.-Y. Zhao, W.-J. Sun, J. Wang, J.-H. He, H. Li, Q.-F. Xu, N.-J. Li, D.-Y. Chen and J.-M. Lu, *Adv. Funct. Mater.*, 2020, **30**, 2004245.
- Y. G. Song, J. M. Suh, J. Y. Park, J. E. Kim, S. Y. Chun, J. U. Kwon, H. Lee, H. W. Jang, S. Kim, C.-Y. Kang and J. H. Yoon, *Adv. Sci.*, 2022, **9**, 2103484.
- H. Xiong, S. Ling, Y. Li, F. Duan, H. Zhu, S. Lu and M. Du, *J. Colloid Interface Sci.*, 2022, **608**, 1126–1134.
- R. Sarpeshkar, *Neural Comput.*, 1998, **10**, 1601–1638.
- H. Chun and T. D. Chung, *Annu. Rev. Anal. Chem.*, 2015, **8**, 441–462.
- M. Onoda, *IEEJ Trans. Electr. Electron. Eng.*, 2020, **15**, 320–334.
- Y. Hou and X. Hou, *Science*, 2021, **373**, 628–629.
- T. Li and K. Xiao, *Adv. Mater. Technol.*, 2022, **7**, 2200205.
- R. J. Sengwa, V. K. Patel and M. Saraswat, *J. Polym. Res.*, 2022, **29**, 480.
- G. Laucirica, M. E. Toimil-Molares, C. Trautmann, W. Marmisoll and O. Azzaroni, *ACS Appl. Mater. Interfaces*, 2020, **12**, 28148–28157.
- P. Zhang, W. Guo, Z. H. Guo, Y. Ma, L. Gao, Z. Cong, X. J. Zhao, L. Qiao, X. Pu and Z. L. Wang, *Adv. Mater.*, 2021, **33**, 2101396.
- J. Yu, Y. Wang, S. Qin, G. Gao, C. Xu, Z. L. Wang and Q. Sun, *Mater. Today*, 2022, **60**, 158–182.
- J. Zhang, W. Liu, J. Dai and K. Xiao, *Adv. Sci.*, 2022, **9**, 2200534.
- A. Zhang and C. M. Lieber, *Chem. Rev.*, 2016, **116**, 215–257.
- Y. Lee, J. Park, A. Choe, S. Cho, J. Kim and H. Ko, *Adv. Funct. Mater.*, 2020, **30**, 1904523.
- C. Yang and Z. Suo, *Nat. Rev. Mater.*, 2018, **3**, 125–142.
- K. Raidongia and J. Huang, *J. Am. Chem. Soc.*, 2012, **134**, 16528–16531.
- P. Jia, L. Wang, Y. Zhang, Y. Yang, X. Jin, M. Zhou, D. Quan, M. Jia, L. Cao, R. Long, L. Jiang and W. Guo, *Adv. Mater.*, 2021, **33**, 2007529.
- H. Kim, M. Kim, A. Lee, H.-L. Park, J. Jang, J.-H. Bae, I. M. Kang, E.-S. Kim and S.-H. Lee, *Adv. Sci.*, 2023, **10**, 19.
- S.-H. Lee, H.-L. Park, C.-M. Keum, I.-H. Lee, M.-H. Kim and S.-D. Lee, *Phys. Status Solidi RRL*, 2019, **13**, 1900044.
- S.-H. Lee, H.-L. Park, M.-H. Kim, S. Kang and S.-D. Lee, *ACS Appl. Mater. Interfaces*, 2019, **11**, 30108–30115.
- J. Li, Y. Qian, W. Li, S. Yu, Y. Ke, H. Qian, Y.-H. Lin, C.-H. Hou, J.-J. Shyue, J. Zhou, Y. Chen, J. Xu, J. Zhu, M. Yi and W. Huang, *Adv. Mater.*, 2023, **35**, 23.
- J. Meng, Z. Li, Y. Fang, Q. Li, Z. He, T. Wang, H. Zhu, L. Ji, Q. Sun, D. W. Zhang and L. Chen, *IEEE Electron Device Lett.*, 2022, **43**, 2069–2072.
- H.-L. Park, M.-H. Kim, M.-H. Kim and S.-H. Lee, *Nanoscale*, 2020, **12**, 22502–22510.
- J. Shi, S. Kang, J. Feng, J. Fan, S. Xue, G. Cai and J. S. Zhao, *Nanoscale Horiz.*, 2023, **8**, 509–515.
- Y. Wang, Y. Gong, L. Yang, Z. Xiong, Z. Lv, X. Xing, Y. Zhou, B. Zhang, C. Su, Q. Liao and S.-T. Han, *Adv. Funct. Mater.*, 2021, **31**, 2100144.
- Y. Pei, L. Yan, Z. Wu, J. Lu, J. Zhao, J. Chen, Q. Liu and X. Yan, *ACS Nano*, 2021, **15**, 17319–17326.
- J.-L. Meng, T.-Y. Wang, Z.-Y. He, L. Chen, H. Zhu, L. Ji, Q.-Q. Sun, S.-J. Ding, W.-Z. Bao, P. Zhou and D. W. Zhang, *Mater. Horiz.*, 2021, **8**, 538–546.
- M. Kumar, Y. H. Ahn, S. Iqbal, U. Kim and H. Seo, *Small*, 2022, **18**, 2105585.
- Y. Li, Y. Pan, C. Zhang, Z. Shi, C. Ma, S. Ling, M. Teng, Q. Zhang, Y. Jiang, R. Zhao and Q. Zhang, *ACS Appl. Mater. Interfaces*, 2022, **14**, 44676–44684.
- Z. Wang, L. Wang, Y. Wu, L. Bian, M. Nagai, R. Jv, L. Xie, H. Ling, Q. Li, H. Bian, M. Yi, N. Shi, X. Liu and W. Huang, *Adv. Mater.*, 2021, **33**, 2104370.



- 39 X. Zhao, J. Xu, D. Xie, Z. Wang, H. Xu, Y. Lin, J. Hu and Y. Liu, *Adv. Mater.*, 2021, **33**, 2104023.
- 40 C. Zhang, Y. Li, F. Yu, G. Wang, K. Wang, C. Ma, X. Yang, Y. Zhou and Q. Zhang, *Nano Energy*, 2023, **109**, 108274.
- 41 C. Zhang, X. Wang, Y. Li, Y. Sun and Q. Zhang, *Chem. – Eur. J.*, 2023, **29**, e202300481.
- 42 H. Patil, H. Kim, K. D. Kadam, S. Rehman, S. A. Patil, J. Aziz, T. D. Dongale, Z. A. Sheikh, M. K. Rahmani, M. F. Khan and D.-K. Kim, *ACS Appl. Mater. Interfaces*, 2023, **15**, 13238–13248.
- 43 X. Wen, W. Tang, Z. Lin, X. Peng, Z. Tang and L. Hou, *Appl. Phys. Lett.*, 2023, **122**, 173301.
- 44 M. Zhang, C. Ma, D. Du, J. Xiang, S. Yao, E. Hu, S. Liu, Y. Tong, W.-Y. Wong and Q. Zhao, *Adv. Electron. Mater.*, 2020, **6**, 2000841.
- 45 H. Yang, Z. Wang, X. Guo, H. Su, K. Sun, D. Yang, W. Xiao, Q. Wang and D. He, *ACS Appl. Mater. Interfaces*, 2020, **12**, 34370–34377.
- 46 D. Goldhaber-Gordon, M. S. Montemerlo, J. C. Love, G. J. Opiteck and J. C. Ellenbogen, *Proc. IEEE*, 1997, **85**, 521–540.
- 47 P. Zhang, M. Xia, F. Zhuge, Y. Zhou, Z. Wang, B. Dong, Y. Fu, K. Yang, Y. Li, Y. He, R. H. Scheicher and X. S. Miao, *Nano Lett.*, 2019, **19**, 4279–4286.
- 48 C. Li, L. Han, H. Jiang, M. H. Jang, P. Lin, Q. Wu, M. Barnell, J. J. Yang, H. L. Xin and Q. Xia, *Nat. Commun.*, 2017, **8**, 15666.
- 49 S. Choi, S. Jang, J.-H. Moon, J. C. Kim, H. Y. Jeong, P. Jang, K.-J. Lee and G. Wang, *NPG Asia Mater.*, 2018, **10**, 1097–1106.
- 50 S. Kim, S. Jung, M. H. Kim, Y. C. Chen, Y. F. Chang, K. C. Ryoo, S. Cho, J. H. Lee and B. G. Park, *Small*, 2018, **14**, 1704062.
- 51 F. Wan, Q. Wang, T. Harumoto, T. Gao, K. Ando, Y. Nakamura and J. Shi, *Adv. Funct. Mater.*, 2020, **30**, 2007101.
- 52 M. Ali, A. Sokolov, M. J. Ko and C. Choi, *J. Alloys Compd.*, 2021, **855**, 157514.
- 53 Q. Liao, Y. Wang, Z. Lv, Z. Xiong, J. Chen, G. P. Wang, S.-T. Han and Y. Zhou, *Org. Electron.*, 2021, **90**, 106062.
- 54 J. Chen, Z. Feng, M. Luo, J. Wang, Z. Wang, Y. Gong, S. Huang, F. Qian, Y. Zhou and S.-T. Han, *J. Mater. Chem. C*, 2021, **9**, 15435–15444.
- 55 U. Das, P. Sarkar, B. Paul and A. Roy, *Appl. Phys. Lett.*, 2021, **118**, 182103.
- 56 A. S. Sokolov, M. Ali, R. Riaz, Y. Abbas, M. J. Ko and C. Choi, *Adv. Funct. Mater.*, 2019, **29**, 1807504.
- 57 K.-H. Son and H.-S. Lee, *Appl. Surf. Sci.*, 2022, **575**, 151754.
- 58 K. Sun, Q. Wang, L. Zhou, J. Wang, J. Chang, R. Guo, B. K. Tay and X. Yan, *Sci. China Mater.*, 2023, **66**, 2013–2022.
- 59 C. Wang, Z. Si, X. Jiang, A. Malik, Y. Pan, S. Stathopoulos, A. Serb, S. Wang, T. Prodromakis and C. Papavassiliou, *IEEE J. Emerging Sel. Top. Circuits*, 2022, **12**, 723–734.
- 60 X. Yang, B. Taylor, A. Wu, Y. Chen and L. O. Chua, *IEEE T. Circuits-I*, 2022, **69**, 1845–1857.
- 61 H. Liao, J. Chen, L. Lan, Y. Yu, G. Zhu, J. Duan, X. Zhu, H. Dai, M. Xiao, Z. Li, W. Yue and I. McCulloch, *ACS Appl. Mater. Interfaces*, 2022, **14**, 16477–16486.
- 62 J. Qiu, D. Zeng, Y. Lin, W. Ye, C. Chen, Z. Xu, G. Hu and Y. Liu, *Spectrochim. Acta, Part A*, 2023, **285**, 121913.
- 63 H. Niu, M. Ding, X. Li, X. Su, X. Han, N. Zhang, P. Guan and X. Hu, *Mater. Chem. Phys.*, 2023, **293**, 126971.
- 64 Y. Yuan, B. Wang, K. Xue, Y. Ma, X. Liu, X. Peng, M. Liu and H. Lu, *ACS Appl. Mater. Interfaces*, 2023, **15**, 17144–17151.
- 65 H. Cheng and J. Ouyang, *J. Phys. Chem. Lett.*, 2022, **13**, 10830–10842.
- 66 A. Wolny and A. Chrobok, *Molecules*, 2022, **27**, 5900.
- 67 M. Zunita, R. Hastuti, A. Alamsyah, G. T. M. Kadja, K. Khoiruddin, K. A. Kurnia, B. Yulianto and I. G. Wenten, *J. Ind. Eng. Chem.*, 2022, **113**, 96–123.
- 68 H. Lv, L. Wei, S. Guo, X. Zhang, F. Chen, X. Qin, C. Wei, B. Jiang and Y. Gong, *Front. Chem.*, 2022, **10**, 807088.
- 69 J. Fu, J.-Y. Liu, G.-H. Zhang, Q.-H. Zhu, S.-L. Wang, S. Qin, L. He and G.-H. Tao, *Small*, 2023, 2302570.
- 70 M. Lee, M.-S. Kim, J.-M. Oh, J. K. Park and S.-M. Paek, *ACS Nano*, 2023, **17**, 3019–3036.
- 71 S. F. Zhao, W. H. Ran, Z. Lou, L. L. Li, S. Poddar, L. L. Wang, Z. Y. Fan and G. Z. Shen, *Natl. Sci. Rev.*, 2022, **9**, nwac158.
- 72 F. Sheng, B. Wu, X. Li, T. Xu, M. A. Shehzad, X. Wang, L. Ge, H. Wang and T. Xu, *Adv. Mater.*, 2021, **33**, 2104404.
- 73 C. Zhang, Y. Li, Y. Zhou, Q. Zhang, H. Li and J. Lu, *Chem. Commun.*, 2018, **54**, 10610–10613.
- 74 C. Yu, J.-H. He, X.-F. Cheng, H.-Z. Lin, H. Yu and J.-M. Lu, *Angew. Chem., Int. Ed.*, 2021, **60**, 15328–15334.
- 75 X. Xiao, X.-F. Cheng, X. Hou, J.-H. He, Q.-F. Xu, H. Li, N.-J. Li, D.-Y. Chen and J.-M. Lu, *Small*, 2017, **13**, 1602190.
- 76 J. Zhou, X.-F. Cheng, B.-J. Gao, C. Yu, J.-H. He, Q.-F. Xu, H. Li, N.-J. Li, D.-Y. Chen and J.-M. Lu, *Small*, 2019, **15**, 1803896.
- 77 C. Yu, H.-Z. Lin, J. Zhou, X.-F. Cheng, J.-H. He, H. Li, Q.-F. Xu, N.-J. Li, D.-Y. Chen and J.-M. Lu, *J. Mater. Chem. A*, 2020, **8**, 1052–1058.
- 78 J. Zhou, H. Lin, X.-F. Cheng, J. Shu, J.-H. He, H. Li, Q.-F. Xu, N.-J. Li, D.-Y. Chen and J.-M. Lu, *Mater. Horiz.*, 2019, **6**, 554–562.
- 79 H. Yuan, H. Shimotani, A. Tsukazaki, A. Ohtomo, M. Kawasaki and Y. Iwasa, *J. Am. Chem. Soc.*, 2010, **132**, 6672–6678.
- 80 P. Bhunia, E. Hwang, M. Min, J. Lee, S. Seo, S. Some and H. Lee, *Chem. Commun.*, 2012, **48**, 913–915.
- 81 K. Rajan, A. Chiappone, D. Perrone, S. Bocchini, I. Roppolo, K. Bejtka, M. Castellino, C. F. Pirri, C. Ricciardi and A. Chiolerio, *RSC Adv.*, 2016, **6**, 94128–94138.
- 82 Y. Li, Y. Song, X. Zhang, X. Wu, F. Wang and Z. Wang, *Macromol. Chem. Phys.*, 2015, **216**, 113–121.

- 83 L. Dou, J. Gao, E. Richard, J. You, C. C. Chen, K. C. Cha, Y. He, G. Li and Y. Yang, *J. Am. Chem. Soc.*, 2012, **134**, 10071–10079.
- 84 Z. Zhang, Y. Nie, W. Hua, J. Xu, C. Ban, F. Xiu and J. Liu, *RSC Adv.*, 2020, **10**, 20900–20904.
- 85 D. Wi, J. Kim, H. Lee, N.-G. Kang, J. Lee, M.-J. Kim, J.-S. Lee and M. Ree, *J. Mater. Chem. C*, 2016, **4**, 2017–2027.
- 86 C. Zhang, Y.-T. Tai, J. Shang, G. Liu, K.-L. Wang, C. Hsu, X. Yi, X. Yang, W. Xue, H. Tan, S. Guo, L. Pan and R.-W. Li, *J. Mater. Chem. C*, 2016, **4**, 3217–3223.
- 87 L. Zhao, W. Wu, X. Shen, Q. Liu, Y. He, K. Song, H. Li and Z. Chen, *ACS Appl. Mater. Interfaces*, 2019, **11**, 47073–47082.
- 88 Y. He, X. Hou, Y. Liu and N. Feng, *J. Mater. Chem. B*, 2019, **7**, 5602–5619.
- 89 Z. Yao, L. Pan, L. Liu, J. Zhang, Q. Lin, Y. Ye, Z. Zhang, S. Xiang and B. Chen, *Sci. Adv.*, 2019, **5**, eaaw4515.
- 90 C. S. Dash, S. Sahoo and S. R. S. Prabaharan, *Solid State Ionics*, 2018, **324**, 218–225.
- 91 C. Yun, M. Webb, W. Li, R. Wu, M. Xiao, M. Hellenbrand, A. Kursumovic, H. Dou, X. Gao, S. Dhole, D. Zhang, A. Chen, J. Shi, K. H. L. Zhang, H. Wang, Q. Jia and J. L. MacManus-Driscoll, *J. Mater. Chem. C*, 2021, **9**, 4522–4531.
- 92 M. Kim, M. A. Rehman, D. Lee, Y. Wang, D. H. Lim, M. F. Khan, H. Choi, Q. Y. Shao, J. Suh, H. S. Lee and H. H. Park, *ACS Appl. Mater. Interfaces*, 2022, **14**, 44561–44571.
- 93 X.-F. Cheng, E.-B. Shi, X. Hou, J. Shu, J.-H. He, H. Li, Q.-F. Xu, N.-J. Li, D.-Y. Chen and J.-M. Lu, *Adv. Electron. Mater.*, 2017, **3**, 1700107.
- 94 C. Zhang, Y. Li, Z. Li, Y. Jiang, J. Zhang, R. Zhao, J. Zou, Y. Wang, K. Wang, C. Ma and Q. Zhang, *ACS Appl. Mater. Interfaces*, 2022, **14**, 3111–3120.
- 95 Q. Lu, Y. Xia, F. Sun, Y. Shi, Y. Zhao, S. Wang and T. Zhang, *Adv. Mater. Technol.*, 2023, 2300059.
- 96 B. Sun, S. Ranjan, G. Zhou, T. Guo, C. Du, L. Wei, Y. N. Zhou and Y. A. Wu, *ACS Appl. Electron. Mater.*, 2021, **3**, 2380–2388.
- 97 Z. Zhao, Q. Che, K. Wang, M. E. El-Khouly, J. Liu, Y. Fu, B. Zhang and Y. Chen, *iScience*, 2022, **25**, 103640.
- 98 T. S. Badessa and V. A. Shaposhnik, *Electrochim. Acta*, 2017, **231**, 453–459.
- 99 G. Cho, Y. Park, Y.-K. Hong and D.-H. Ha, *Nano Converg.*, 2019, **6**, 17.
- 100 I. Bejanidze, O. Petrov, V. Pohrebennyk, T. Kharebava, N. Nakashidze, N. Didmanidze, N. Davitadze and A. Petrov, *Appl. Sci.*, 2020, **10**, 7383.
- 101 G. Yilmaz, *Polymers*, 2019, **11**, 1577.
- 102 M. A. Tasdelen, J. Lalevee and Y. Yagci, *Polym. Chem.*, 2020, **11**, 1111–1121.
- 103 L. Breloy, O. Yavuz, I. Yilmaz, Y. Yagci and D.-L. Versace, *Polym. Chem.*, 2021, **12**, 4291–4316.
- 104 K. Luo, H. Chen, Q. Zhou, Z. Yan, Z. Su and K. Li, *Spectrochim. Acta, Part A*, 2021, **247**, 119046.
- 105 Y. Li, C. Li, B. Wang, W. Li and P. Che, *J. Alloys Compd.*, 2019, **772**, 770–774.
- 106 F. Li, J. Lu, Q. Zhang, D. Peng, Z. Yang, Q. Xu, C. Pan, A. Pan, T. Li and R. Wang, *Sci. Bull.*, 2019, **64**, 698–704.
- 107 S. A. Kurnosenko, O. I. Silyukov, A. S. Mazur and I. A. Zvereva, *Ceram. Int.*, 2020, **46**, 5058–5068.
- 108 G. G. Warr and R. Atkin, *Curr. Opin. Colloid Interface Sci.*, 2020, **45**, 83–96.
- 109 B. Shi, D. Shen, W. Li and G. Wang, *Macromol. Rapid Commun.*, 2022, **43**, 2200071.
- 110 Y. Zhong, J. Wang and Y. Tian, *MRS Bull.*, 2019, **44**, 183–188.
- 111 Z. Zhou, J. Zhao, A. P. Chen, Y. Pei, Z. Xiao, G. Wang, J. Chen, G. Fu and X. Yan, *Mater. Horiz.*, 2020, **7**, 1106–1114.
- 112 S. Pan, L. Liu, Q. Huang, J. He, H. Wang and S. Chang, *Sci. China: Phys., Mech. Astron.*, 2023, **66**, 276811.
- 113 A. A. Gismatulin, O. M. Orlov, V. A. Gritsenko and G. Y. Krasnikov, *Chaos, Solitons Fractals*, 2021, **142**, 203502.
- 114 F. Pan, S. Gao, C. Chen, C. Song and F. Zeng, *Mater. Sci. Eng., R*, 2014, **83**, 1–59.
- 115 J.-Q. Yang, R. Wang, Z.-P. Wang, Q.-Y. Ma, J.-Y. Mao, Y. Ren, X. Yang, Y. Zhou and S.-T. Han, *Nano Energy*, 2020, **74**, 104828.
- 116 Y. P. Santos, E. Valenca, R. Machado and M. A. Macedo, *Mater. Sci. Semicond. Process.*, 2018, **86**, 43–48.
- 117 S. Zhu, B. Sun, G. Zhou, C. Ke, T. Guo, H. Zhao, F. Yang, Y. Zhang, Y. A. Wu and Y. Zhao, *Mater. Today Chem.*, 2022, **26**, 101169.
- 118 Y. Zhang, S. Fan, Q. Niu, F. Han and Y. Zhang, *Sci. China Mater.*, 2022, **65**, 3096–3104.
- 119 Y. Wang, J. Yang, W. Ye, D. She, J. Chen, Z. Lv, V. A. L. Roy, H. Li, K. Zhou, Q. Yang, Y. Zhou and S.-T. Han, *Adv. Electron. Mater.*, 2020, **6**, 1900765.
- 120 L. Zhao, J. Xu, X. Shang, X. Li, Q. Li and S. Li, *R. Soc. Open Sci.*, 2019, **6**, 181098.
- 121 Y. Gong, Y. Wang, R. Li, J.-Q. Yang, Z. Lv, X. Xing, Q. Liao, J. Wang, J. Chen, Y. Zhou and S.-T. Han, *J. Mater. Chem. C*, 2020, **8**, 2985–2992.
- 122 Z. Zhou, H. Mao, X. Wang, T. Sun, Q. Chang, Y. Chen, F. Xiu, Z. Liu, J. Liu and W. Huang, *Nanoscale*, 2018, **10**, 14824–14829.
- 123 J. Wang, X.-F. Cheng, W.-H. Qian, Y.-Y. Zhao, J.-H. He, Q.-F. Xu, H. Li, D.-Y. Chen, N.-J. Li and J.-M. Lu, *J. Mater. Chem. C*, 2020, **8**, 7658–7662.
- 124 D. Wang, S. Zhao, L. Li, L. Wang, S. Cui, S. Wang, Z. Lou and G. Shen, *Adv. Funct. Mater.*, 2022, **32**, 2200241.
- 125 S. G. Kim, J. S. Han, H. Kim, S. Y. Kim and H. W. Jang, *Adv. Mater. Technol.*, 2018, **3**, 1800457.
- 126 C. Zhang, H. Li, Y. Su, F. Yu, C. Li, Q. Zhang and J. Lu, *Mater. Chem. Front.*, 2020, **4**, 3280–3289.
- 127 Y. Chen, H. Wei, Y. Wu, T. Yang and B. Cao, *J. Mater. Chem. C*, 2022, **10**, 17386–17397.
- 128 J. Wei, J. Li, C. Yu, Q. Sun, J. He and J. Lu, *Chin. Chem. Lett.*, 2021, **32**, 2463–2468.

- 129 T. R. Desai, S. S. Kundale, T. D. Dongale and C. Gurnani, *ACS Appl. Bio Mater.*, 2023, **6**, 1763–1773.
- 130 X. Li, L. Zhang, R. Guo, J. Chen and X. Yan, *Adv. Mater. Technol.*, 2020, **5**, 2000191.
- 131 M. Saha, S. M. Nawaz, B. K. Keshari and A. Mallik, *ACS Appl. Bio Mater.*, 2022, **5**, 833–840.
- 132 N. Sharma, K. Singh, C. C. Tripathi and M. K. Bera, *J. Electron. Mater.*, 2023, **52**, 3264–3280.
- 133 Q. Xue, Y. Peng, L. Cao, Y. Xia, J. Liang, C. C. Chen, M. Li and T. Hang, *ACS Appl. Mater. Interfaces*, 2022, **14**, 25710–25721.
- 134 J. H. Cha, S. Y. Yang, J. Oh, S. Choi, S. Park, B. C. Jang, W. Ahn and S. Y. Choi, *Nanoscale*, 2020, **12**, 14339–14368.
- 135 C. Zhang, Y. Li, C. Ma and Q. Zhang, *Small Sci.*, 2021, **2**, 2100086.
- 136 L. Cai, L. Yu, W. Yue, Y. Zhu, Z. Yang, Y. Li, Y. Tao and Y. Yang, *Adv. Electron. Mater.*, 2023, **9**, 2300021.
- 137 Z. Liu, J. Tang, B. Gao, P. Yao, X. Li, D. Liu, Y. Zhou, H. Qian, B. Hong and H. Wu, *Nat. Commun.*, 2020, **11**, 4234.
- 138 S. H. Sung, Y. Jeong, J. W. Oh, H.-J. Shin, J. H. Lee and K. J. Lee, *Mater. Today*, 2023, **62**, 251–270.
- 139 W. Huh, D. Lee and C.-H. Lee, *Adv. Mater.*, 2020, **32**, 2002092.
- 140 J. Xu, Y. Huan, K. Yang, Y. Zhan, Z. Zou and L.-R. Zheng, *IEEE Access*, 2018, **6**, 29320–29331.
- 141 R. C. Ivans, S. G. Dahl and K. D. Cantley, *IEEE Trans. Neural Networks Learn. Syst.*, 2020, **31**, 4206–4216.
- 142 J. T. Jang, D. Kim, W. S. Choi, S.-J. Choi, D. M. Kim, Y. Kim and D. H. Kim, *ACS Appl. Electron. Mater.*, 2020, **2**, 2837–2844.
- 143 R. Wang, Z. Mu, H. Sun and Y. Wang, *Front. Phys.*, 2021, 690944.
- 144 Y. Zhou, H. Wu, B. Gao, W. Wu, Y. Xi, P. Yao, S. Zhang, Q. Zhang and H. Qian, *Adv. Funct. Mater.*, 2019, **29**, 1900155.
- 145 Y.-J. Zhang, X.-H. Chen, Z.-R. Wang, Q.-L. Chen, G. Liu, Y. Li, P.-J. Wang, R.-W. Li and X.-S. Miao, *IEEE Trans. Electron Devices*, 2019, **66**, 4710–4715.
- 146 H. Zhao, Z. Liu, J. Tang, B. Gao, Y. Zhang, H. Qian and H. Wu, *Tsinghua Sci. Technol.*, 2022, **27**, 455–471.
- 147 Y. Wang, L. Wu, G. Liu and L. Liu, *J. Alloys Compd.*, 2018, **740**, 273–277.
- 148 S. Wang, X. Dong, Y. Xiong, J. Sha, Y. Cao, Y. Wu, W. Li, Y. Yin and Y. Wang, *Adv. Electron. Mater.*, 2021, **7**, 2100014.
- 149 Y. Li, S. Ling, R. He, C. Zhang, Y. Dong, C. Ma, Y. Jiang, J. Gao, J. He and Q. Zhang, *Nano Res.*, 2023, **16**, 11278–11287.
- 150 C. Zhang, M. Chen, G. Wang, M. Teng, S. Ling, Y. Wang, Z. Su, K. Gao, X. Yang, C. Ma, Y. Li and Q. Zhang, *Chin. J. Chem.*, 2022, **40**, 2296–2304.
- 151 A. H. Jaafar, L. Shao, P. Dai, T. Zhang, Y. Han, R. Beanland, N. T. Kemp, P. N. Bartlett, A. L. Hector and R. Huang, *Nanoscale*, 2022, **14**, 17170–17181.
- 152 C. Zhang, M. Chen, Y. Pan, Y. Li, K. Wang, J. Yuan, Y. Sun and Q. Zhang, *Adv. Sci.*, 2023, **10**, 2207229.
- 153 Y. Li, C. Zhang, Z. Shi, C. Ma, J. Wang and Q. Zhang, *Sci. China Mater.*, 2022, **65**, 2110–2127.
- 154 W. Zhang, H. Gao, C. Deng, T. Lv, S. Hu, H. Wu, S. Xue, Y. Tao, L. Deng and W. Xiong, *Nanoscale*, 2021, **13**, 11497–11504.
- 155 Z. Q. Li, Q. J. Zhang, C. Zhang, H. Li and J. M. Lu, *Org. Electron.*, 2019, **66**, 70–75.
- 156 S. Ling, C. Zhang, C. Ma, Y. Li and Q. Zhang, *Adv. Funct. Mater.*, 2023, **33**, 2208320.
- 157 T. Park, S. S. Kim, B. J. Lee, T. W. Park, H. J. Kim and C. S. Hwang, *Nanoscale*, 2023, **15**, 6387–6395.
- 158 Z. Feng, J. Yu, Y. Wei, Y. Wang, B. Tian, Y. Li, L. Cheng, Z. L. Wang and Q. Sun, *Brain-X*, 2023, **1**, e24.
- 159 B. Tian, Z. Xie, L. Chen, S. Hao, Y. Liu, G. Feng, X. Liu, H. Liu, J. Yang, Y. Zhang, W. Bai, T. Lin, H. Shen, X. Meng, N. Zhong, H. Peng, F. Yue, X. Tang, J. Wang, Q. Zhu, Y. Ivry, B. Dkhil, J. Chu and C. Duan, *Exploration*, 2023, **3**, 20220126.
- 160 Y. Wang, B. Han, M. Mayor and P. Samorì, *Adv. Mater.*, 2023, **30**, 2307359.
- 161 Z. R. Wang, W. B. Zhu, J. H. Li, Y. D. Shao, X. H. Li, H. W. Shi, J. H. Zhao, Z. Y. Zhou, Y. C. Wang and X. B. Yan, *ACS Appl. Mater. Interfaces*, 2023, **15**, 49390–49401.